SUPPLEMENTARY DATA

Design, synthesis, and biological evaluation of new thalidomide-donepezil hybrids as neuroprotective agents targeting cholinesterases and neuroinflammation

Cindy Juliet Cristancho Ortiz[a], Matheus de Freitas Silva[a], Letizia Pruccoli[b], Nathália Fonseca Nadur[c], Luciana Luiza de Azevedo[c], Arthur Eugen Kümmerle[c], Isabella Alvim Guedes[d], Laurent Emmanuel Dardenne[d], Luiz Felipe Leomil Coelho[e], Marcos J. Guimarães[f], Fernanda M. R. da Silva[f], Newton Castro[f], Vanessa Silva Gontijo[a], Viviana C T Rojas[g], Merelym Ketterym de Oliveira[g], Fabiana Cardoso Vilela[g], Alexandre Giusti-Paiva[g], Gisele Barbosa[h], Lídia Moreira Lima[h], Gabriela Beserra Pinheiro[i], Letícia Germino Veras[i], Márcia Renata Mortari[i], Andrea Tarozzi[ab] and Claudio Viegas Jr.*[a]

Table of Contents

IR, NMR and HRMS Spectrum data

All compounds were characterized by IR, NMR and HRMS techniques, also the purity was determined by HPLC. The spectra of the synthesized compounds are shown below

Spectrum data of compounds 3a-h

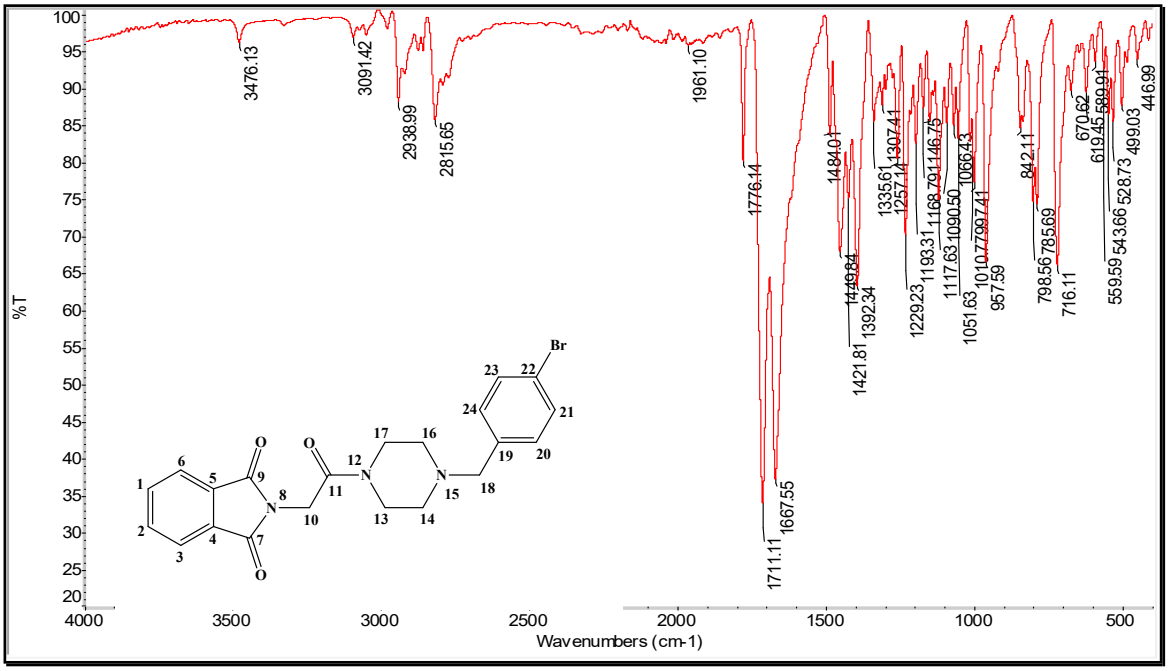

Figure 1. Absorption spectra in the infrared region *2-(2-(4-(4-bromobenzyl)piperazin-1-yl)-2-oxoethyl)isoindoline-1,3-dione* **(3a)** (ATR).

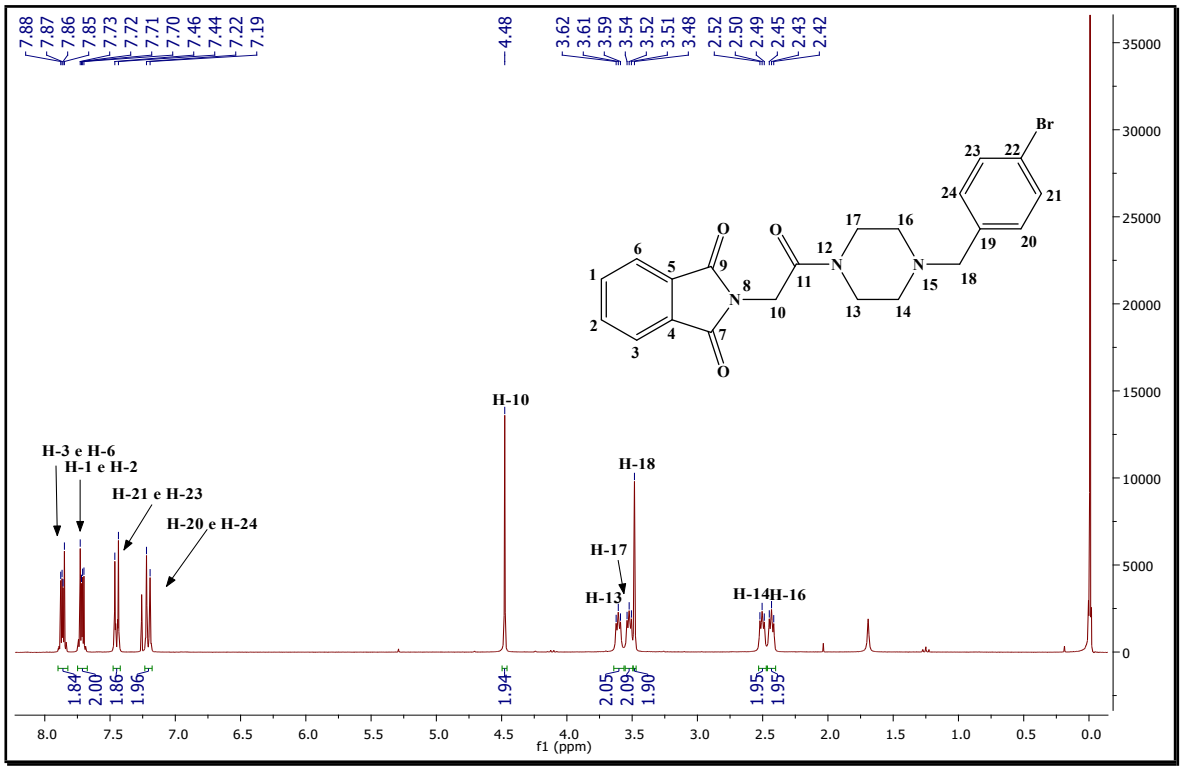

Figure 2. ^{1}H NMR spectra of 2-(2-(4-(4-bromobenzyl)piperazin-1-yl)-2-oxoethyl)isoindoline-1,3-dione **(3a)** (300 MHz, $CDCl_3$).

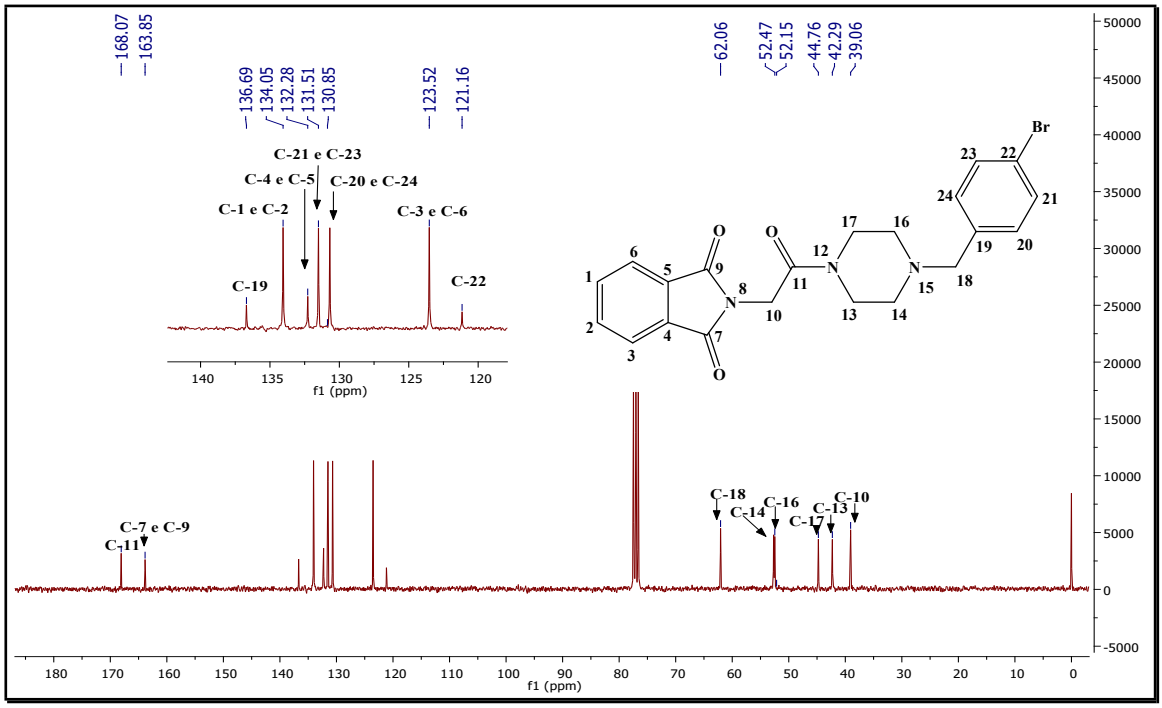

Figure 3. ^{13}C NMR spectra of (E)-3-(4-hydroxy-3-methylphenyl)acrylohydrazide (**6a**) (75 MHz, $CDCl_3$).

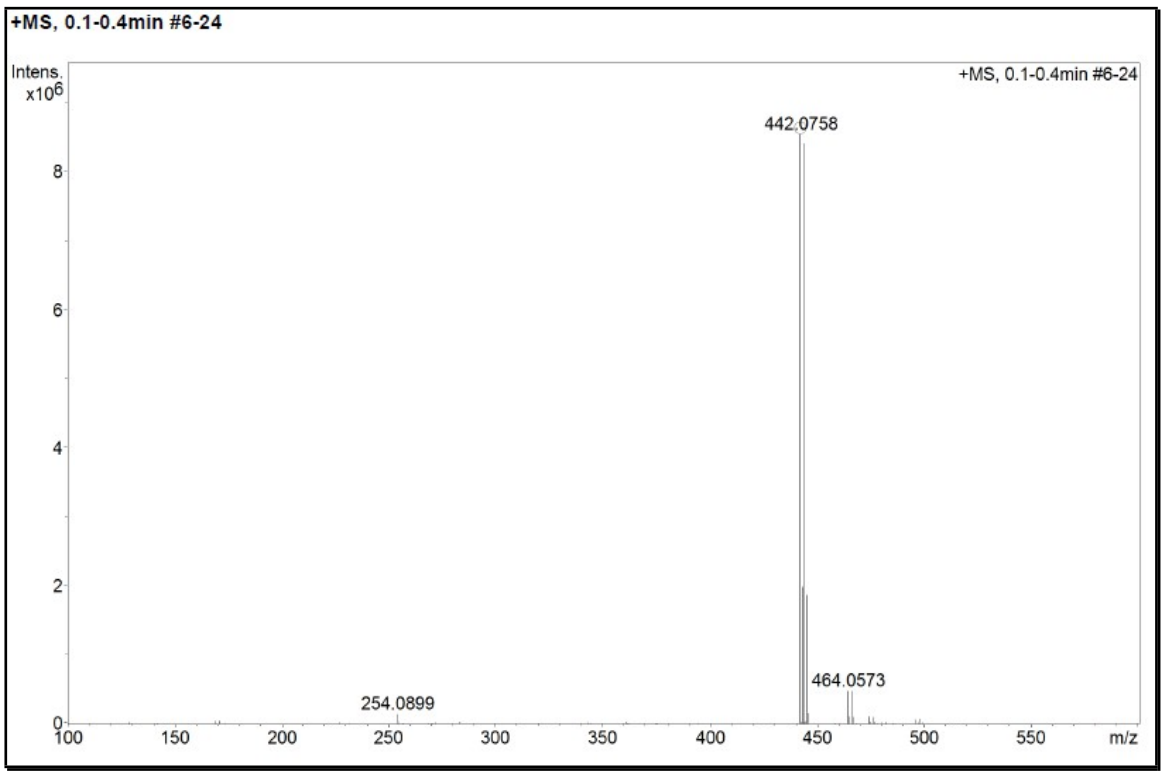

Figure 4. HR-MS spectra of 2-(2-(4-(4-bromobenzyl)piperazin-1-yl)-2-oxoethyl)isoindoline-1,3-dione **(3a)** (ESI-MS).

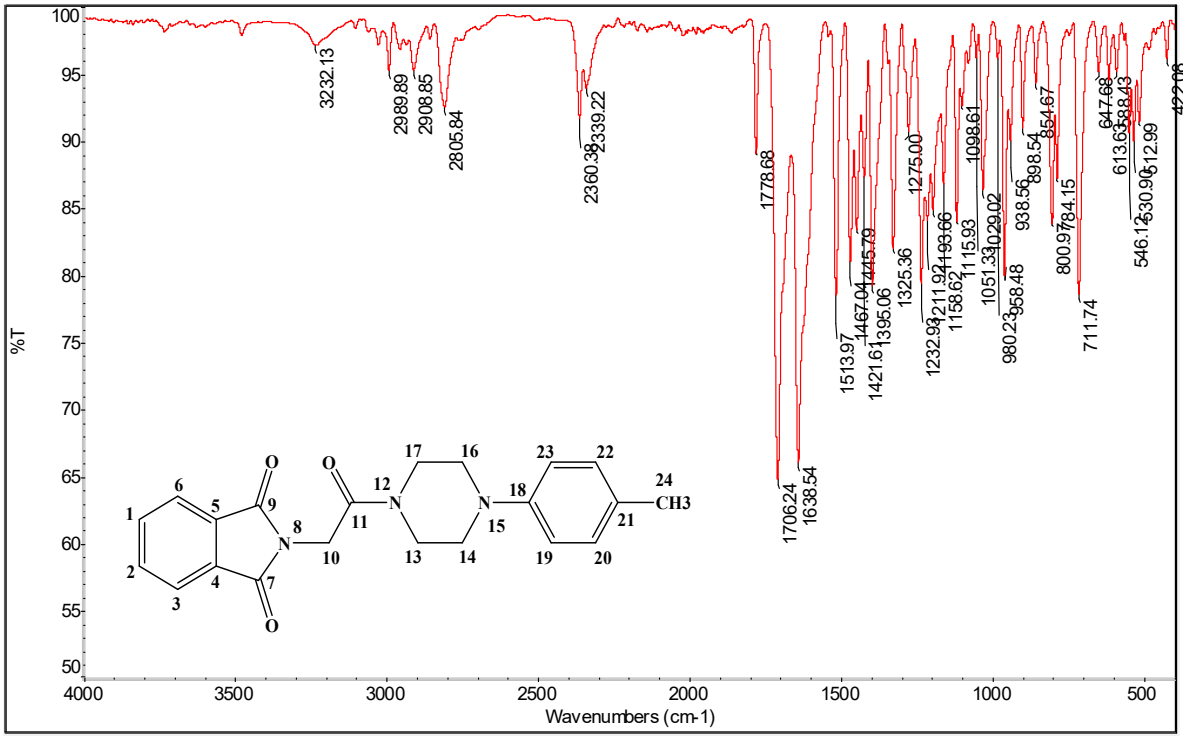

Figure 5. Absorption spectra in the infrared region of *2-(2-oxo-2-(4-(p-tolyl)piperazin-1-yl)ethyl)isoindoline-1,3-dione* **(3b)** (ATR).

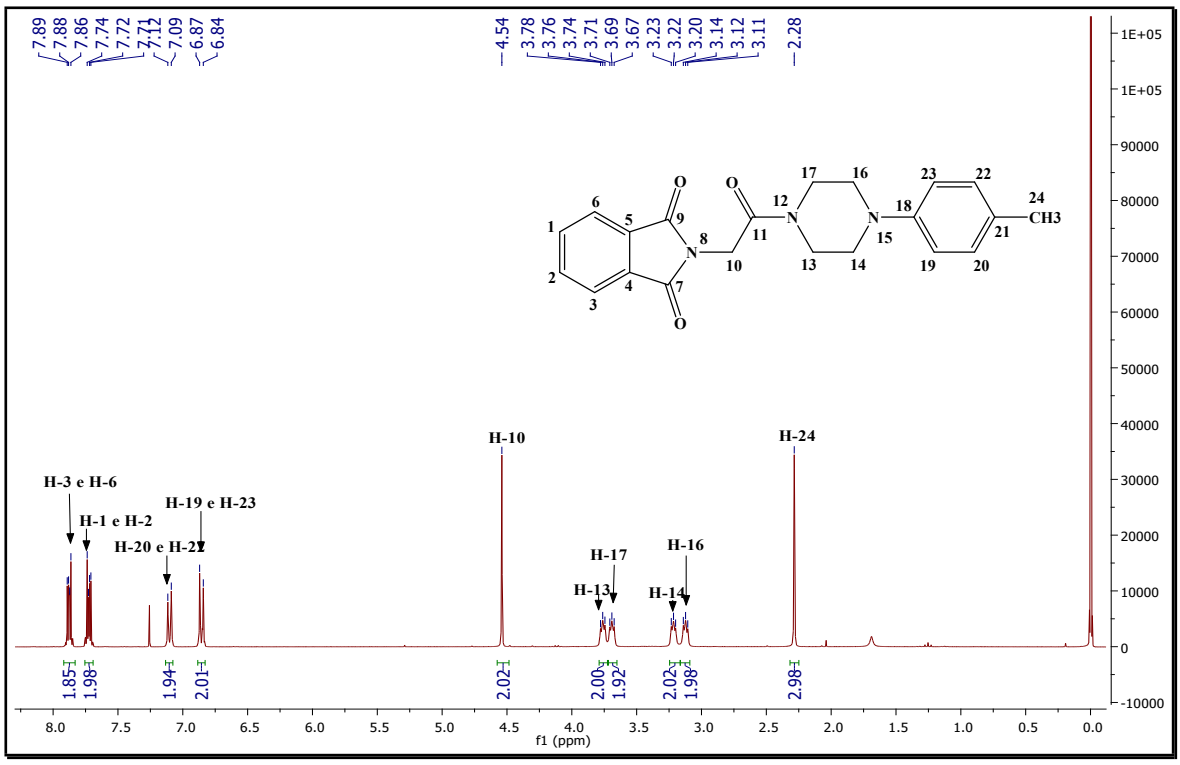

Figure 6. ^{1}H NMR spectra of *2-(2-oxo-2-(4-(p-tolyl)piperazin-1-yl)ethyl)isoindoline-1,3-dione* **(3b)** (300 MHz, $CDCl_3$).

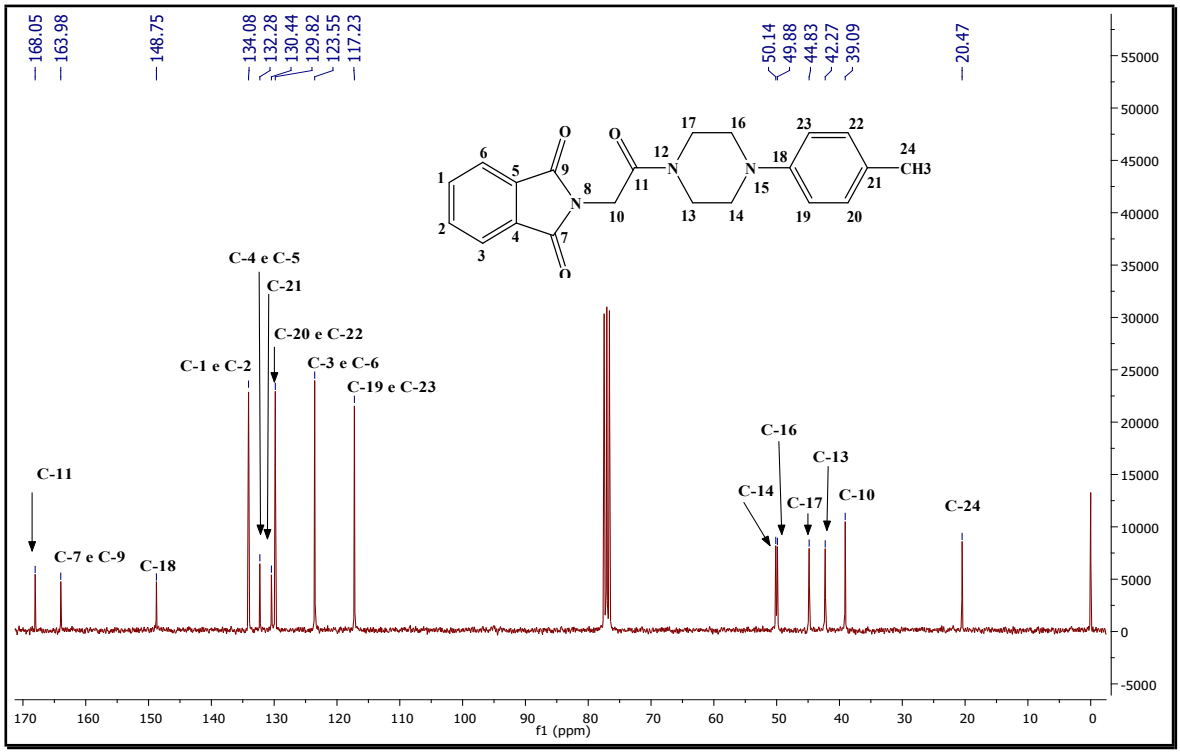

Figure 7. ^{13}C NMR spectra of *2-(2-oxo-2-(4-(p-tolyl)piperazin-1-yl)ethyl)isoindoline-1,3-dione* **(3b)** (75 MHz, $CDCl_3$).

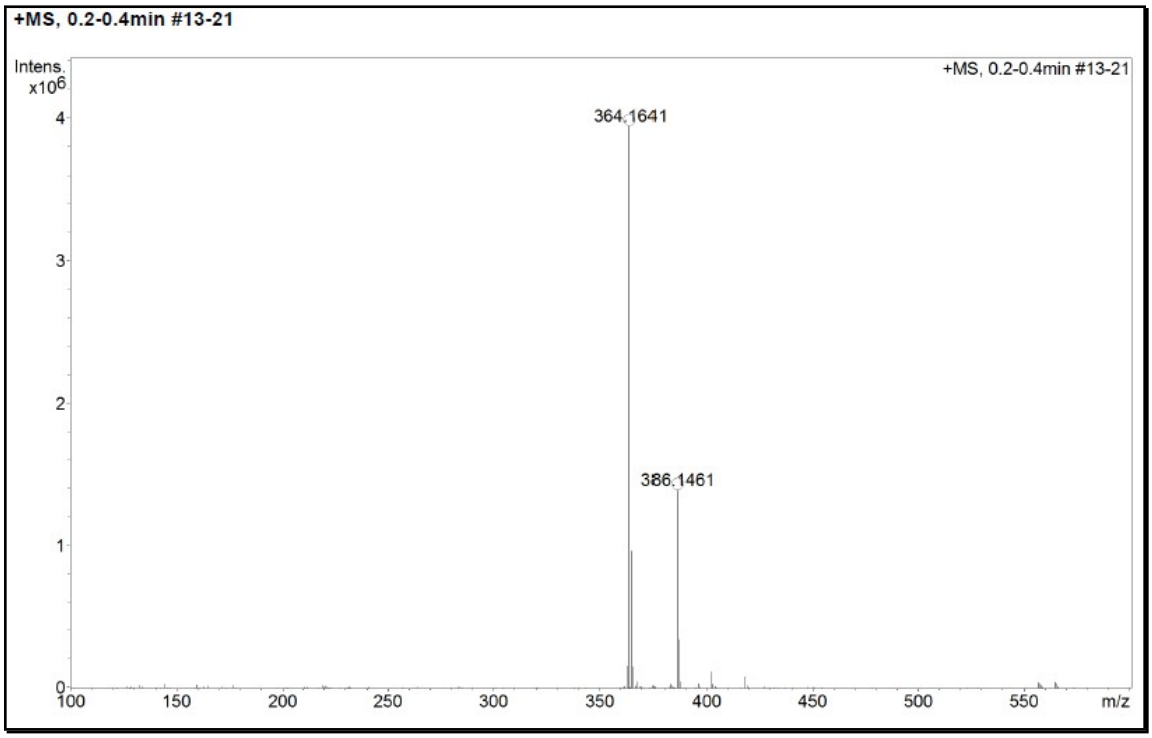

Figure 8. HR-MS spectra of *2-(2-oxo-2-(4-(p-tolyl)piperazin-1-yl)ethyl)isoindoline-1,3-dione* **(3b)** (ESI-MS).

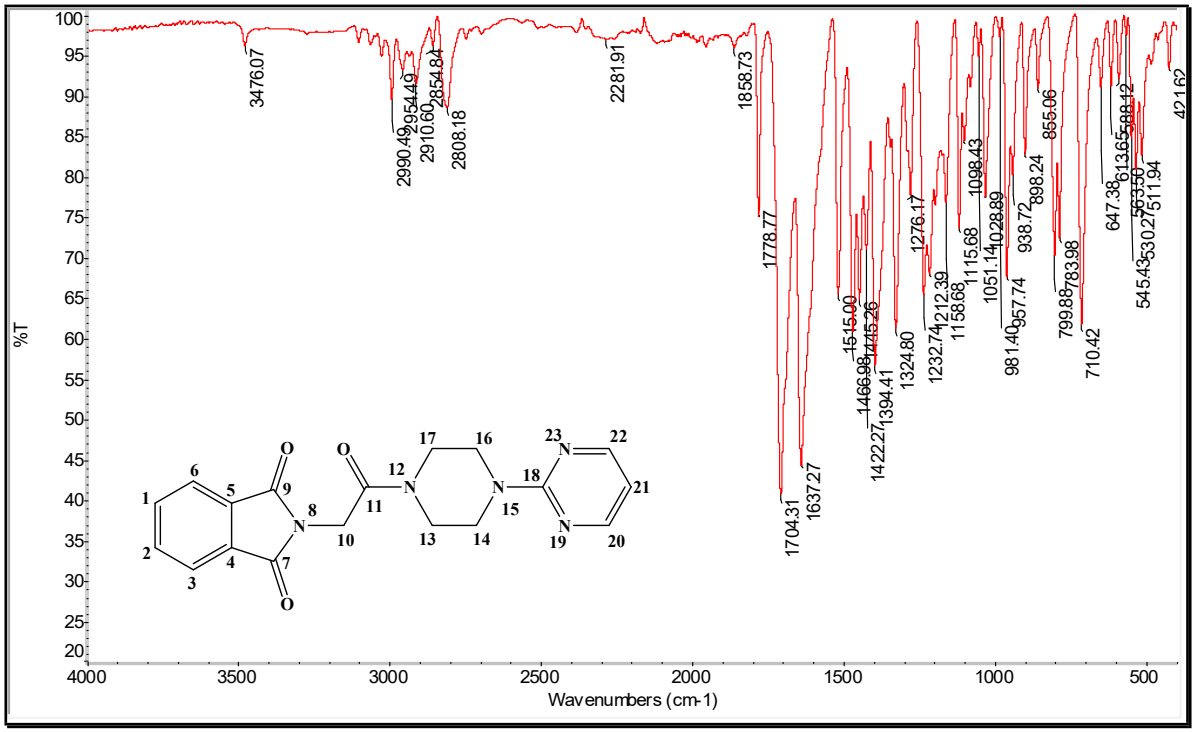

Figure 9. Absorption spectra in the infrared region of *2-(2-oxo-2-(4-(pyrimidin-2-yl)piperazin-1-yl)ethyl)isoindoline-1,3-dione* **(3c)** (ATR).

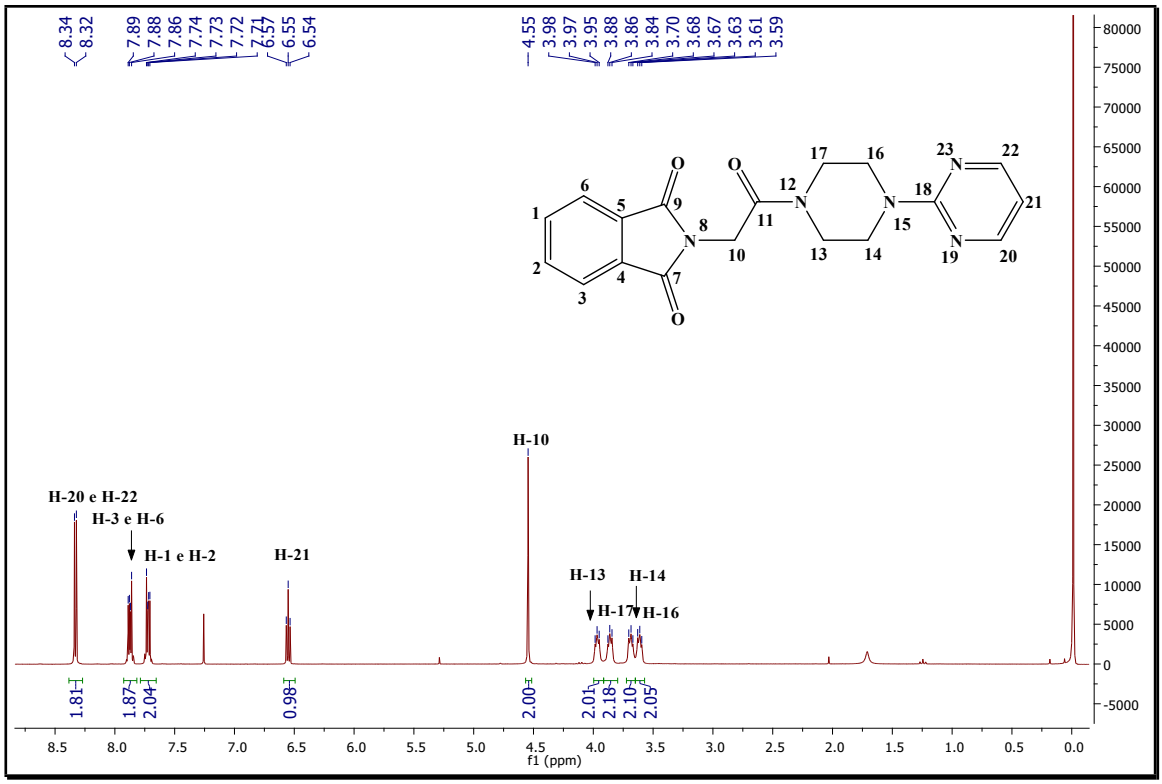

Figure 10. ^{1}H NMR spectra of *2-(2-oxo-2-(4-(pyrimidin-2-yl)piperazin-1-yl)ethyl)isoindoline-1,3-dione* **(3c)** (300 MHz, $CDCl_3$).

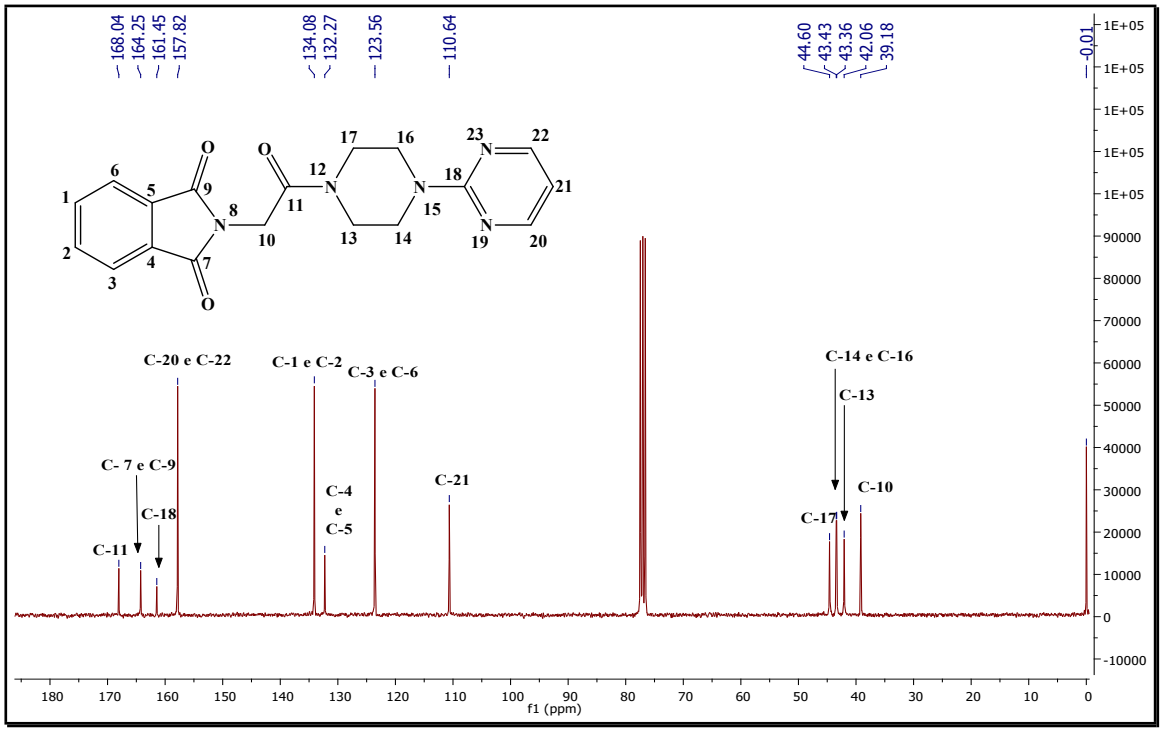

Figure 11. ^{13}C NMR spectra of *2-(2-oxo-2-(4-(pyrimidin-2-yl)piperazin-1-yl)ethyl)isoindoline-1,3-dione* **(3c)** (75 MHz, $CDCl_3$).

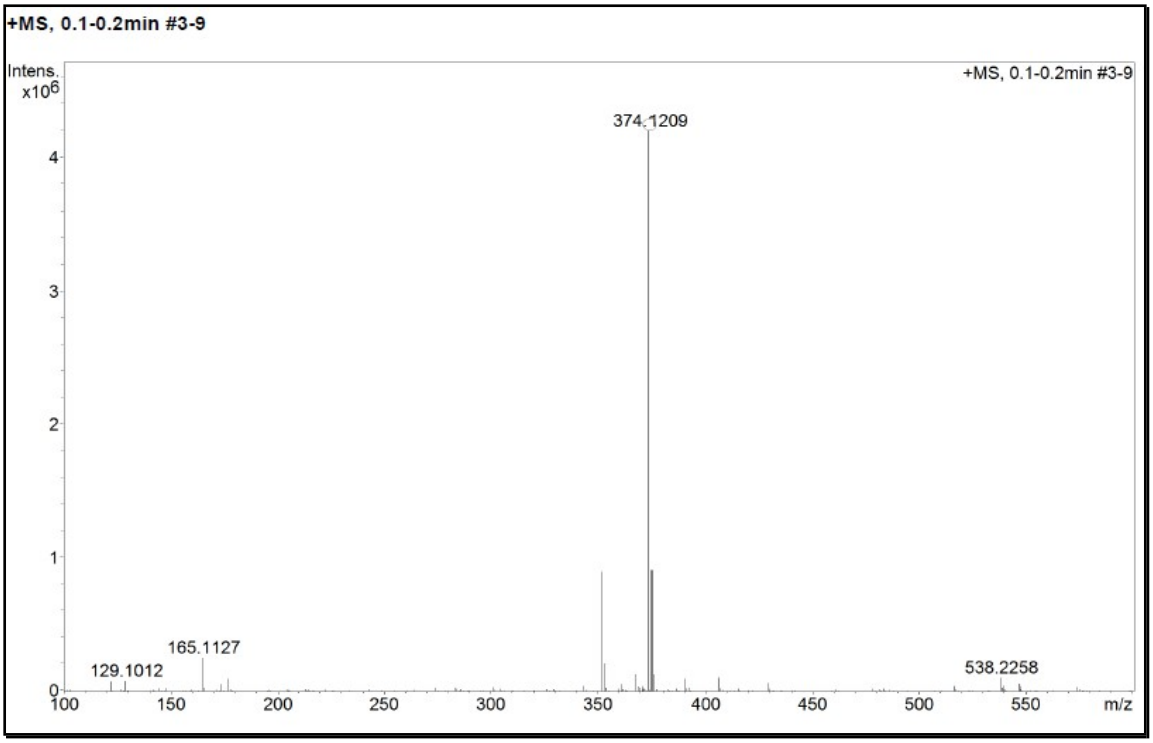

Figure 12. HR-MS spectra of*2-(2-oxo-2-(4-(pyrimidin-2-yl)piperazin-1-yl)ethyl)isoindoline-1,3-dione* **(3c)** (ESI-MS).

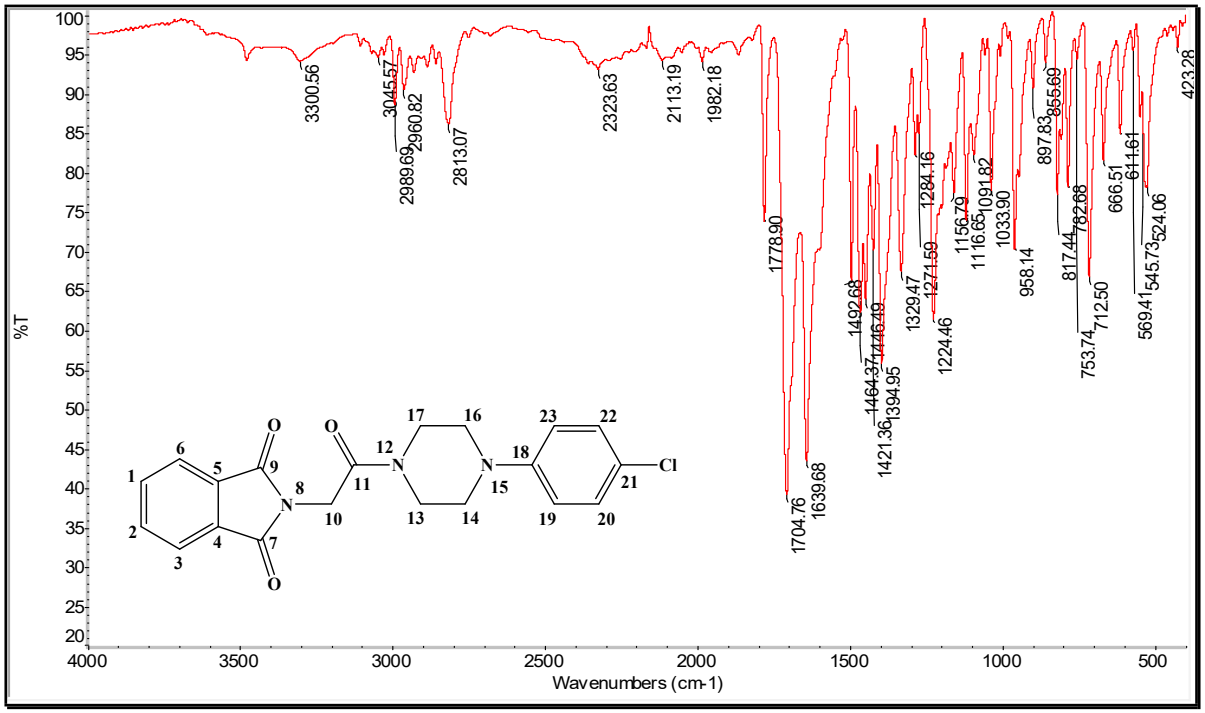

Figure 13. Absorption spectra in the infrared region *of 2-(2-(4-(4-chlorophenyl)piperazin-1-yl)-2-oxoethyl)isoindoline-1,3-dione* **(3d)** (ATR).

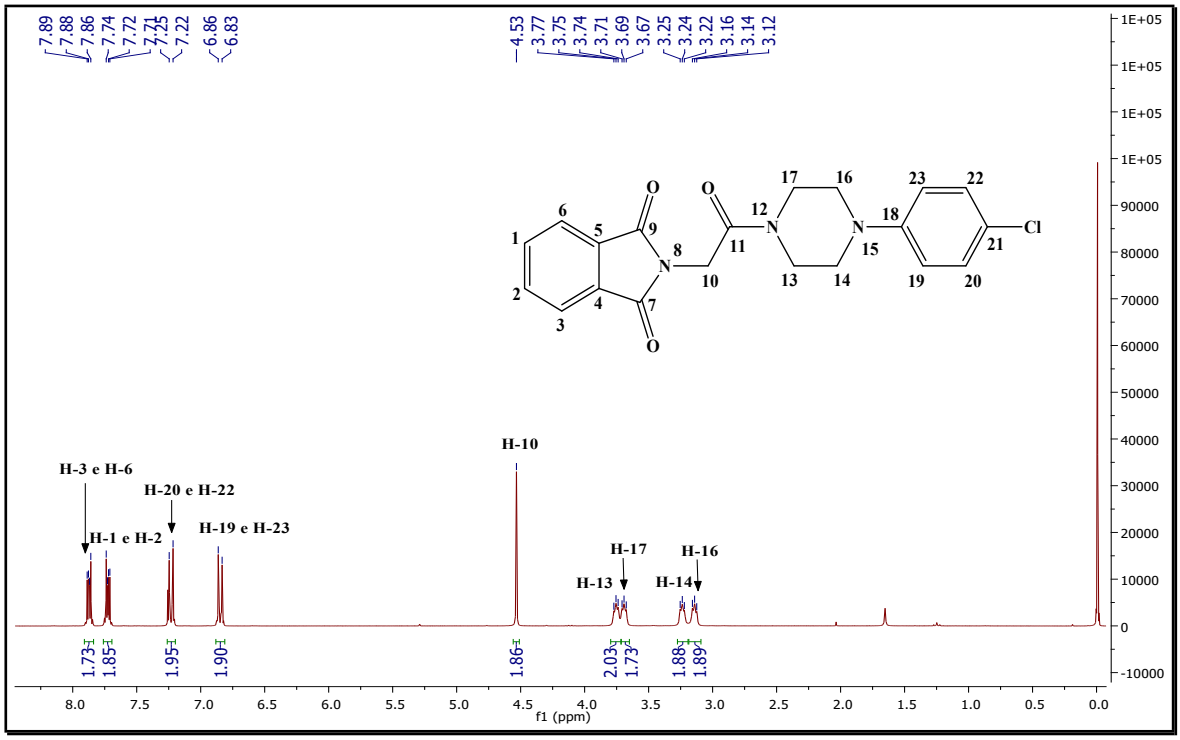

Figure 14. ^{1}H NMR spectra of *2-(2-(4-(4-chlorophenyl)piperazin-1-yl)-2-oxoethyl)isoindoline-1,3-dione* **(3d)** (300 MHz, $CDCl_3$).

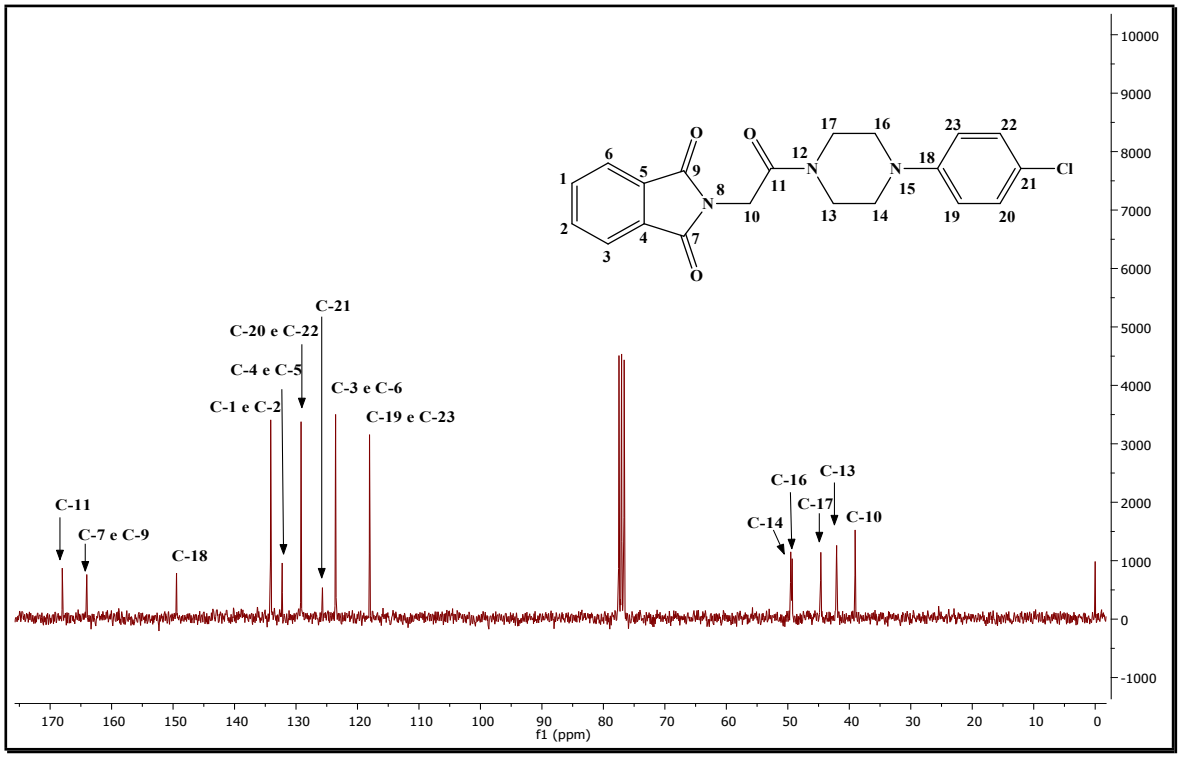

Figure 15. ^{13}C NMR spectra of *2-(2-(4-(4-chlorophenyl)piperazin-1-yl)-2-oxoethyl)isoindoline-1,3-dione* **(3d)** (75 MHz, $CDCl_3$).

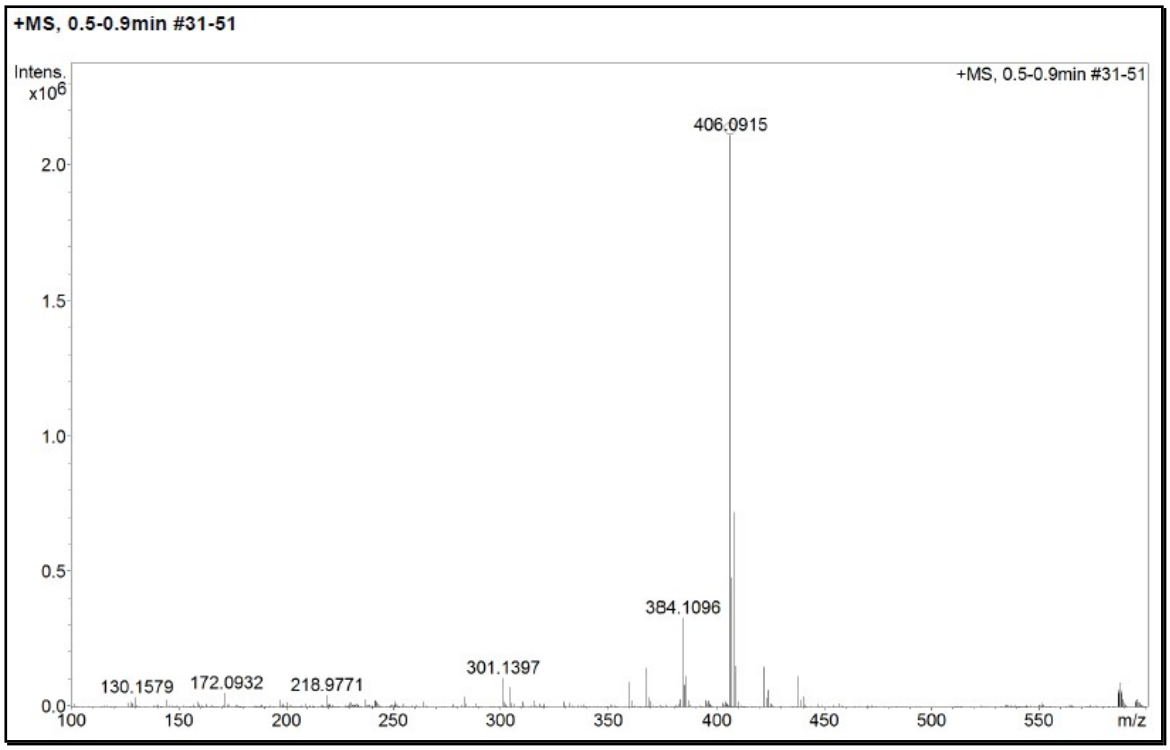

Figure 16. HR-MS spectra of *2-(2-(4-(4-chlorophenyl)piperazin-1-yl)-2-oxoethyl)isoindoline-1,3-dione* **(3d)** (ESI-MS).

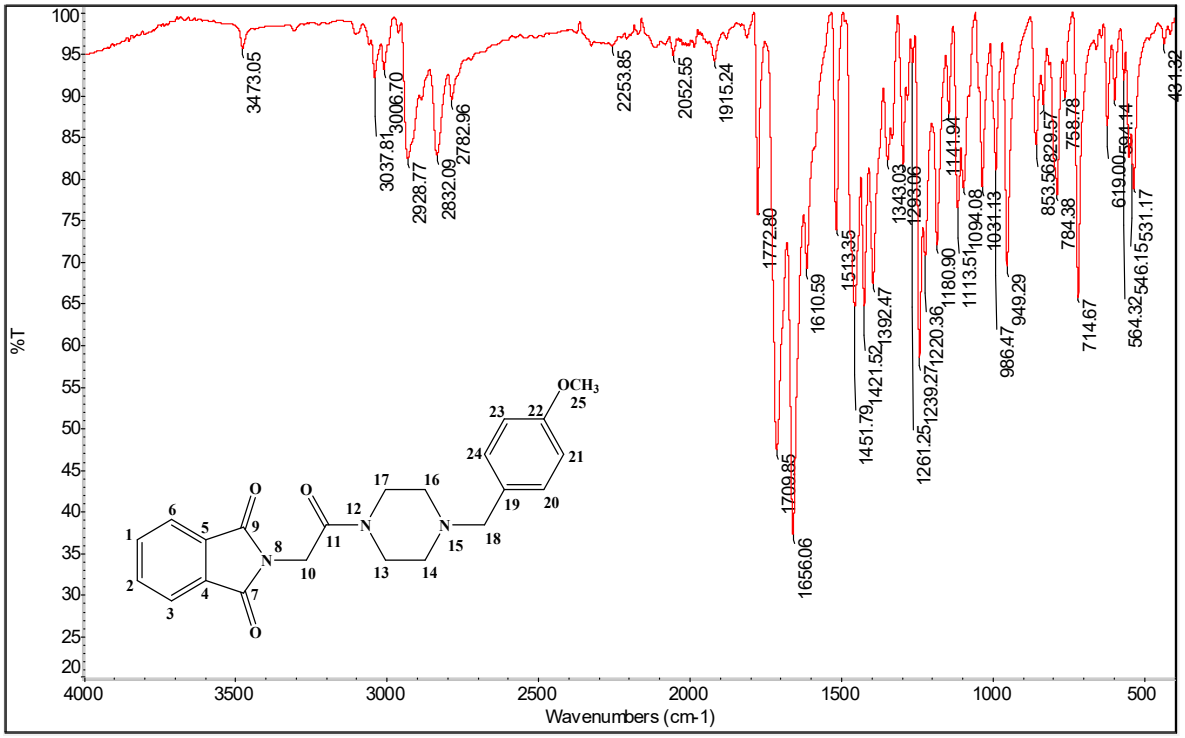

Figure 17. Absorption spectra in the infrared region of *2-(2-(4-(4-methoxybenzyl)piperazin-1-yl)-2-oxoethyl)isoindoline-1,3-dione* **(3e)** (ATR).

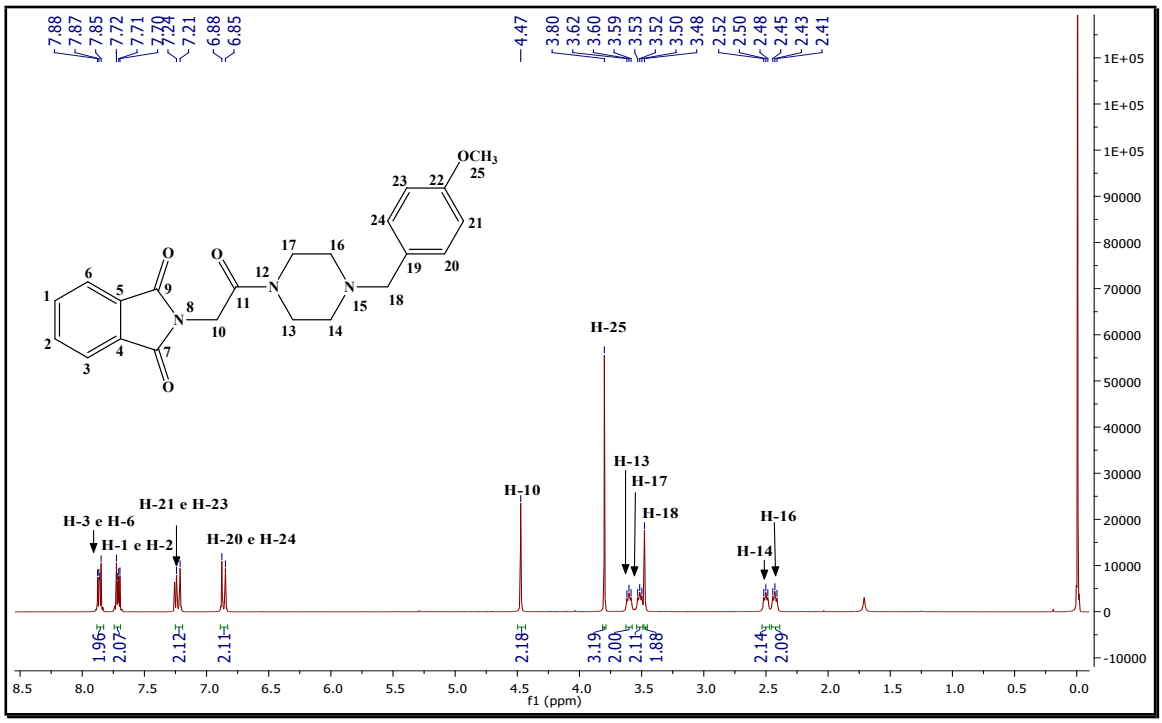

Figure 18. ^{1}H NMR spectra of *2-(2-(4-(4-methoxybenzyl)piperazin-1-yl)-2-oxoethyl)isoindoline-1,3-dione* **(3e)** (300 MHz, $CDCl_3$).

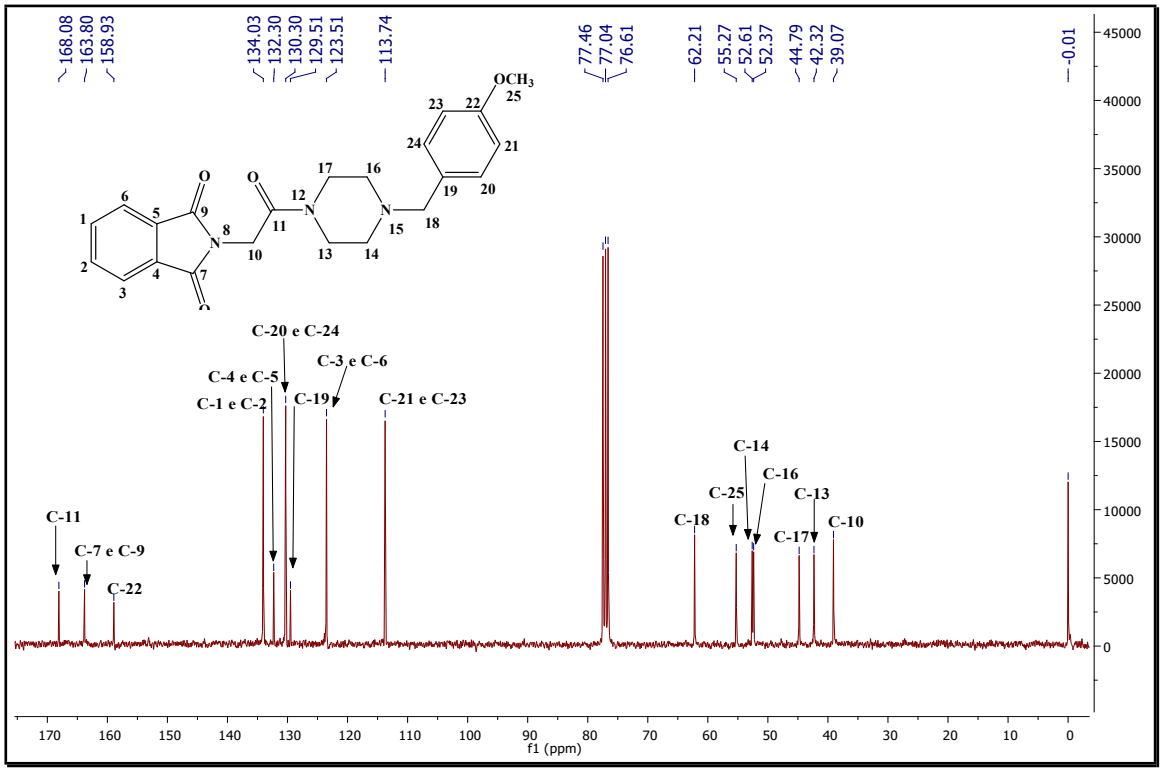

Figure 19. ^{13}C NMR spectra of *2-(2-(4-(4-methoxybenzyl)piperazin-1-yl)-2-oxoethyl)isoindoline-1,3-dione* **(3e)** (75 MHz, $CDCl_3$).

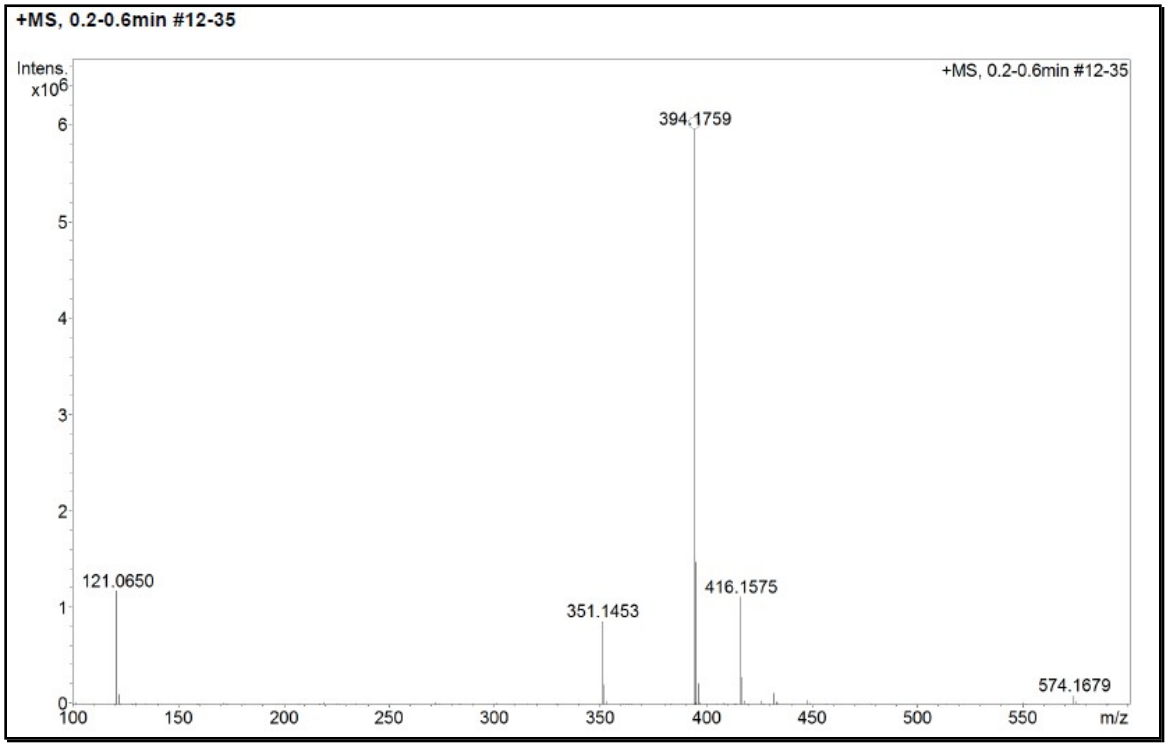

Figure 20. HR-MS spectra of *2-(2-(4-(4-methoxybenzyl)piperazin-1-yl)-2-oxoethyl)isoindoline-1,3-dione* **(3e)** (ESI-MS).

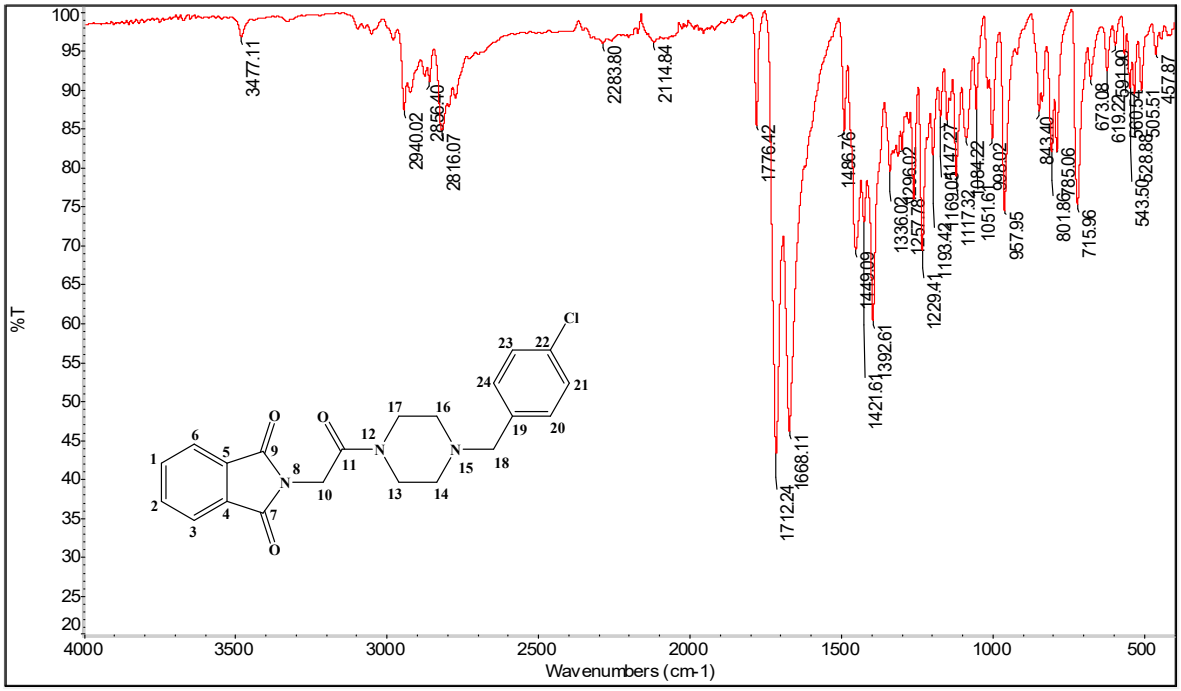

Figure 21. Absorption spectra in the infrared region of *2-(2-(4-(4-chlorobenzyl)piperazin-1-yl)-2-oxoethyl)isoindoline-1,3-dione* **(3f)** (ATR).

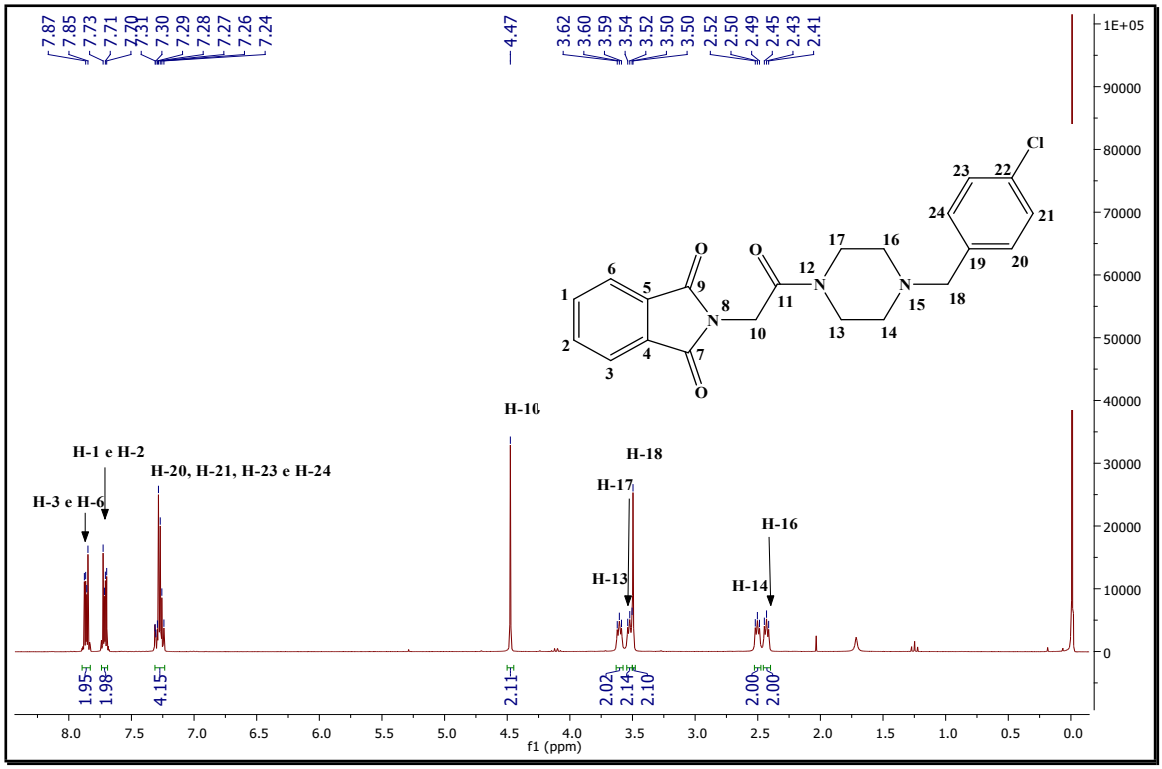

Figure 22. ^{1}H NMR spectra of *2-(2-(4-(4-chlorobenzyl)piperazin-1-yl)-2-oxoethyl)isoindoline-1,3-dione* **(3f)** (300 MHz, $CDCl_3$).

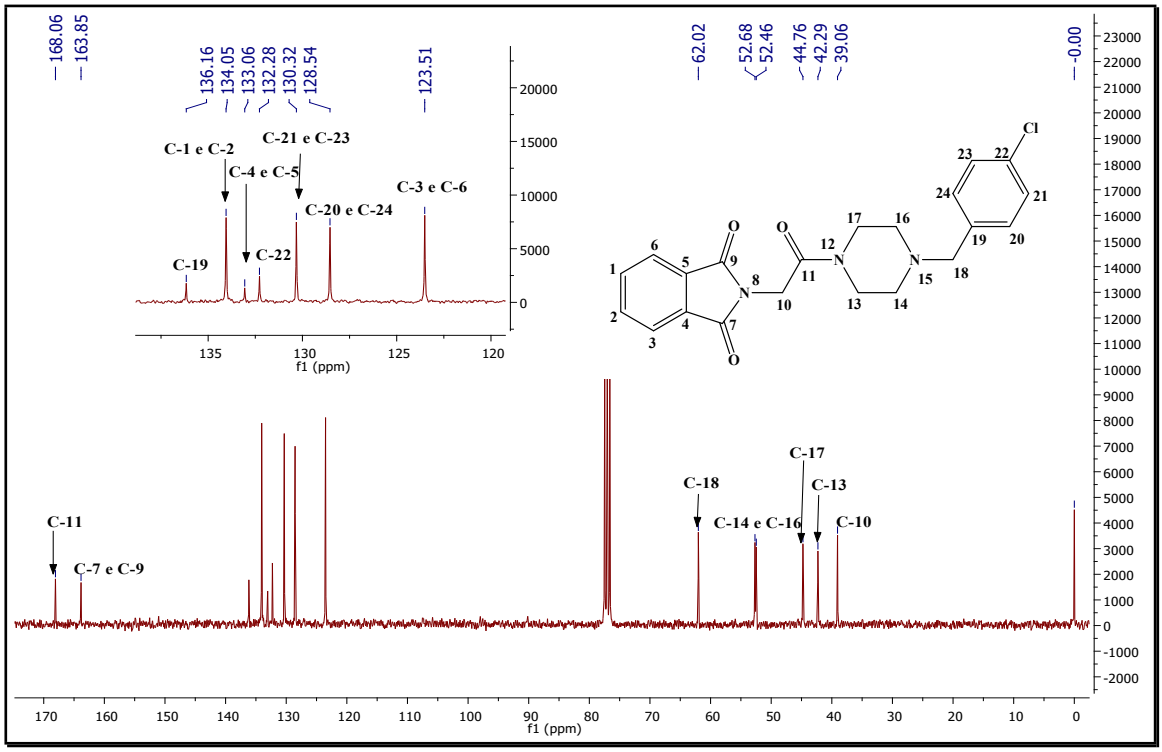

Figure 23. ^{13}C NMR spectra of *2-(2-(4-(4-chlorobenzyl)piperazin-1-yl)-2-oxoethyl)isoindoline-1,3-dione* **(3f)** (75 MHz, $CDCl_3$).

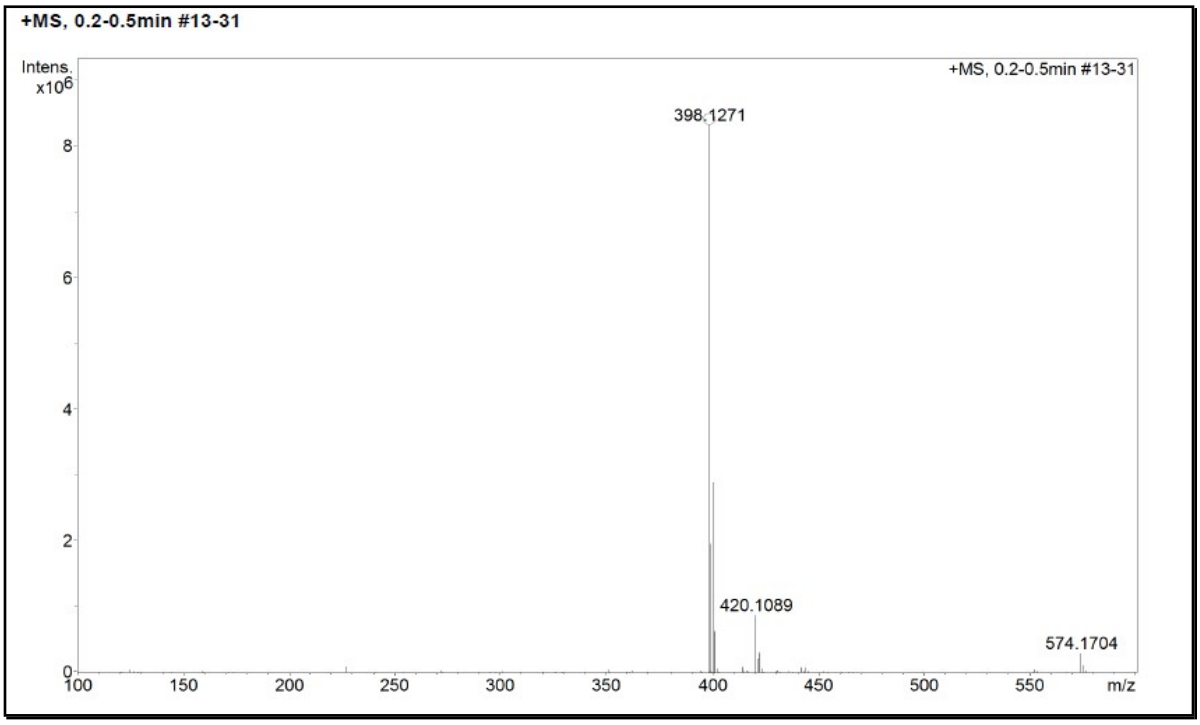

Figure 24. HR-MS spectra of *2-(2-(4-(4-chlorobenzyl)piperazin-1-yl)-2-oxoethyl)isoindoline-1,3-dione* **(3f)** (ESI-MS).

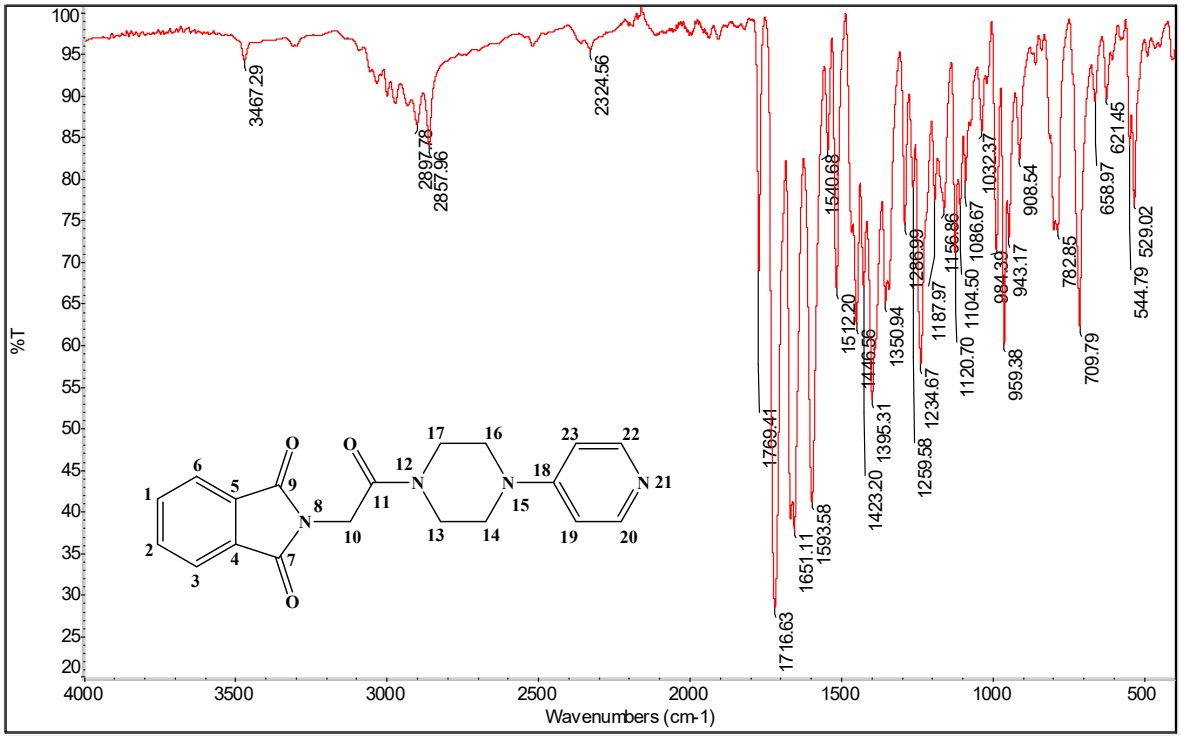

Figure 25. Absorption spectra in the infrared region of *2-(2-oxo-2-(4-(pyridin-4-yl)piperazin-1-yl)ethyl)isoindoline-1,3-dione* **(3g)** (ATR).

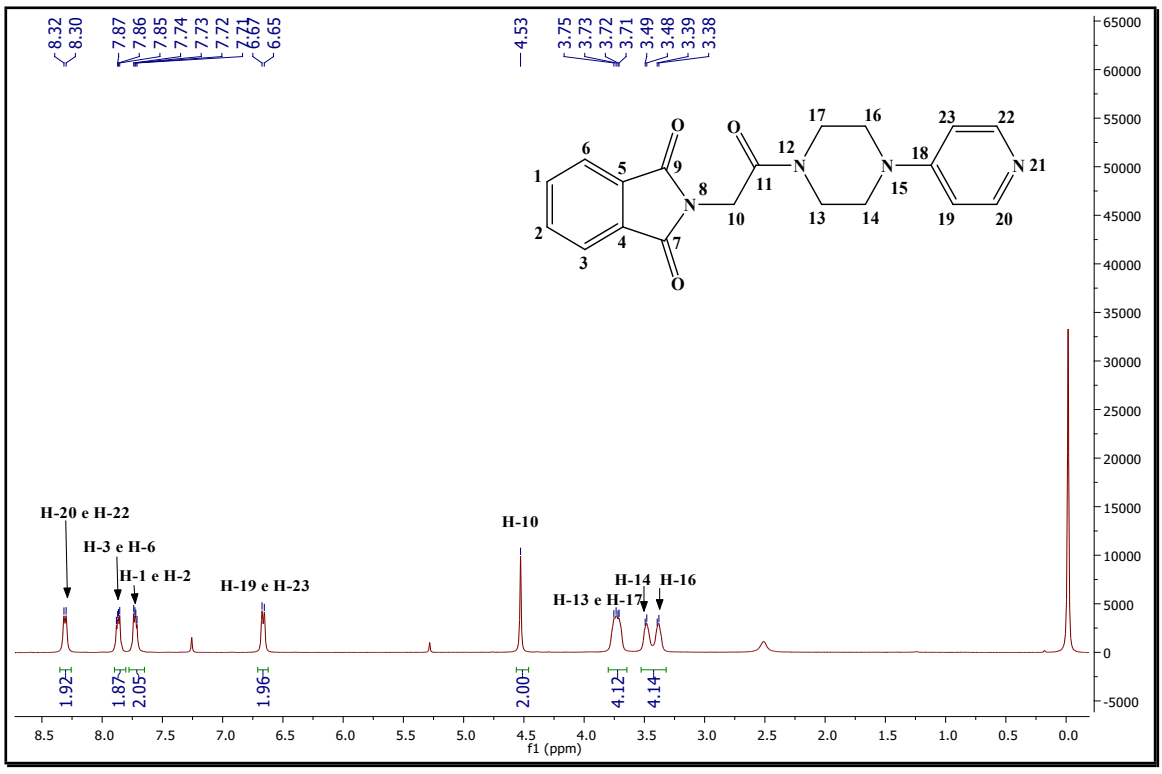

Figure 26. ^{1}H NMR spectra of *2-(2-oxo-2-(4-(pyridin-4-yl)piperazin-1-yl)ethyl)isoindoline-1,3-dione* **(3g)** (300 MHz, $CDCl_3$).

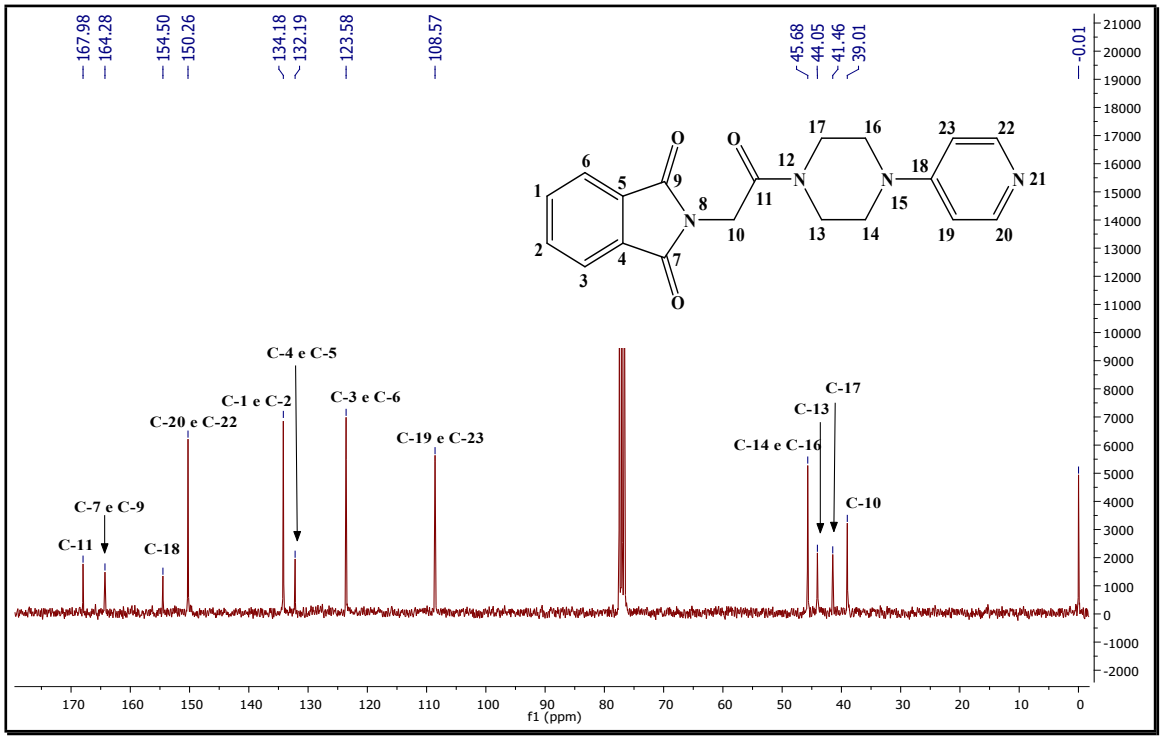

Figure 27. ^{13}C NMR spectra of *2-(2-oxo-2-(4-(pyridin-4-yl)piperazin-1-yl)ethyl)isoindoline-1,3-dione* **(3g)** (75 MHz, $CDCl_3$).

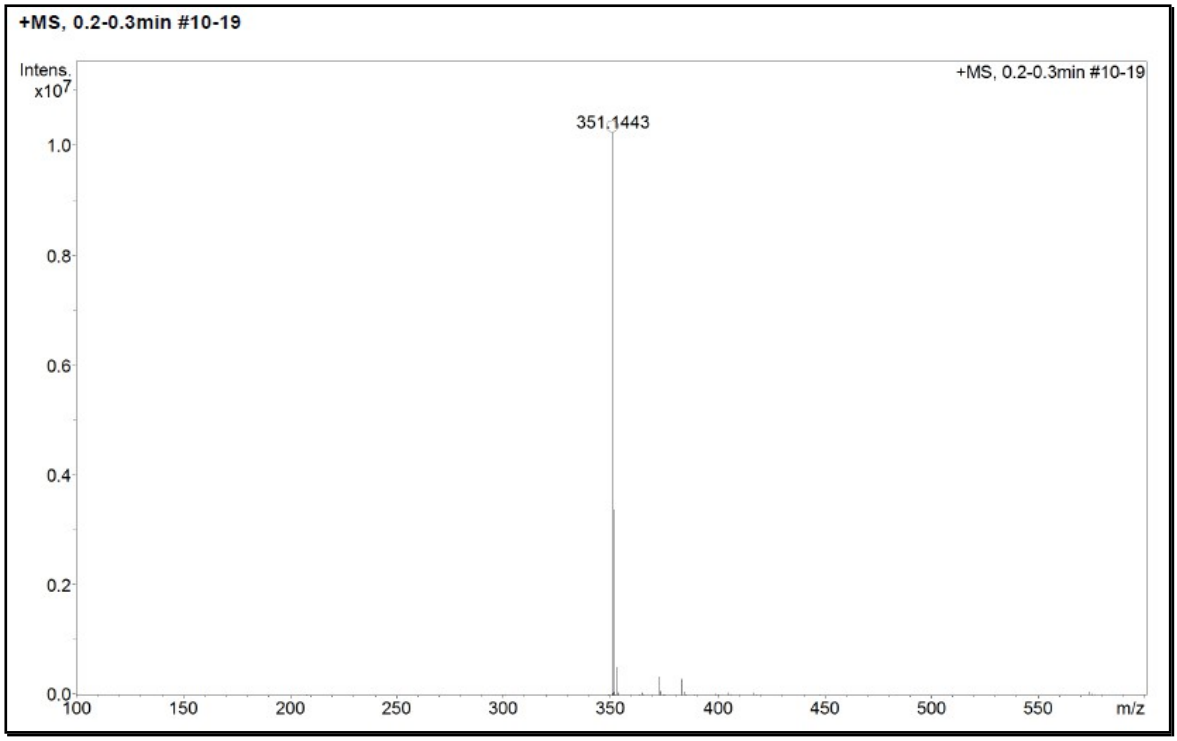

Figure 28. HR-MS spectra of *2-(2-oxo-2-(4-(pyridin-4-yl)piperazin-1-yl)ethyl)isoindoline-1,3-dione* **(3g)** (ESI-MS).

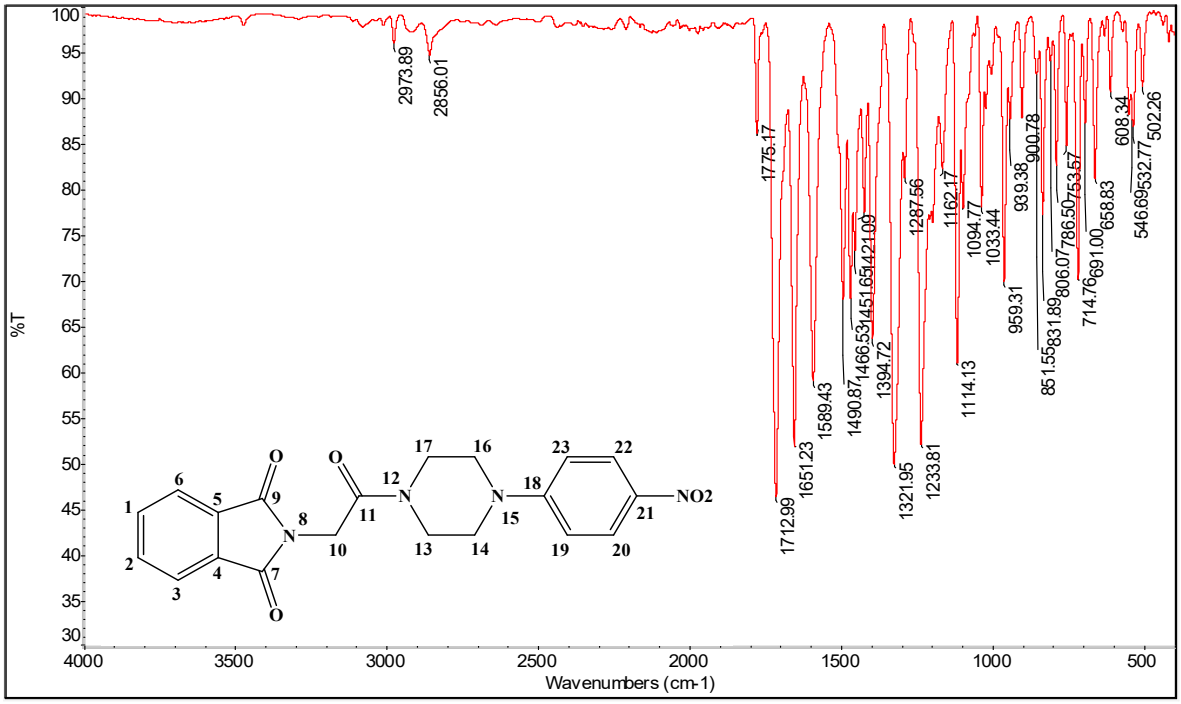

Figure 29. Absorption spectra in the infrared region of *2-(2-(4-(4-nitrophenyl)piperazin-1-yl)-2-oxoethyl)isoindoline-1,3-dione* **(3h)** (ATR).

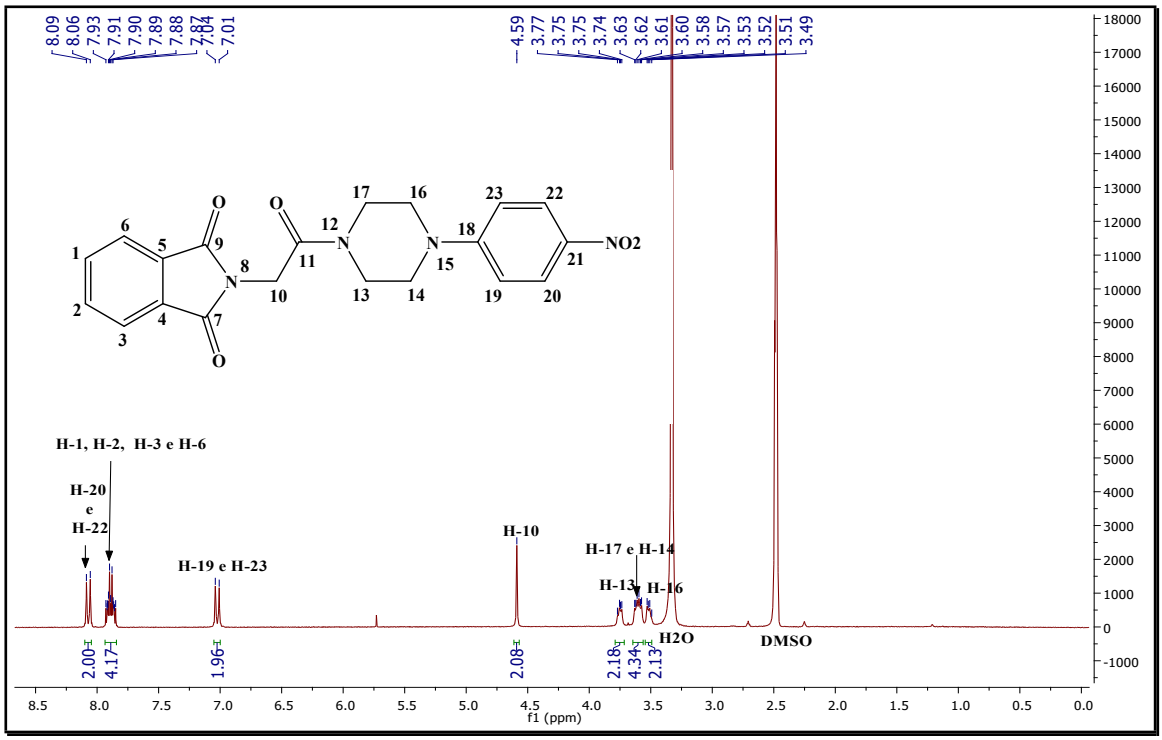

Figure 30. [1]H NMR spectra of *2-(2-(4-(4-nitrophenyl)piperazin-1-yl)-2-oxoethyl)isoindoline-1,3-dione* **(3h)** (300 MHz, DMSO).

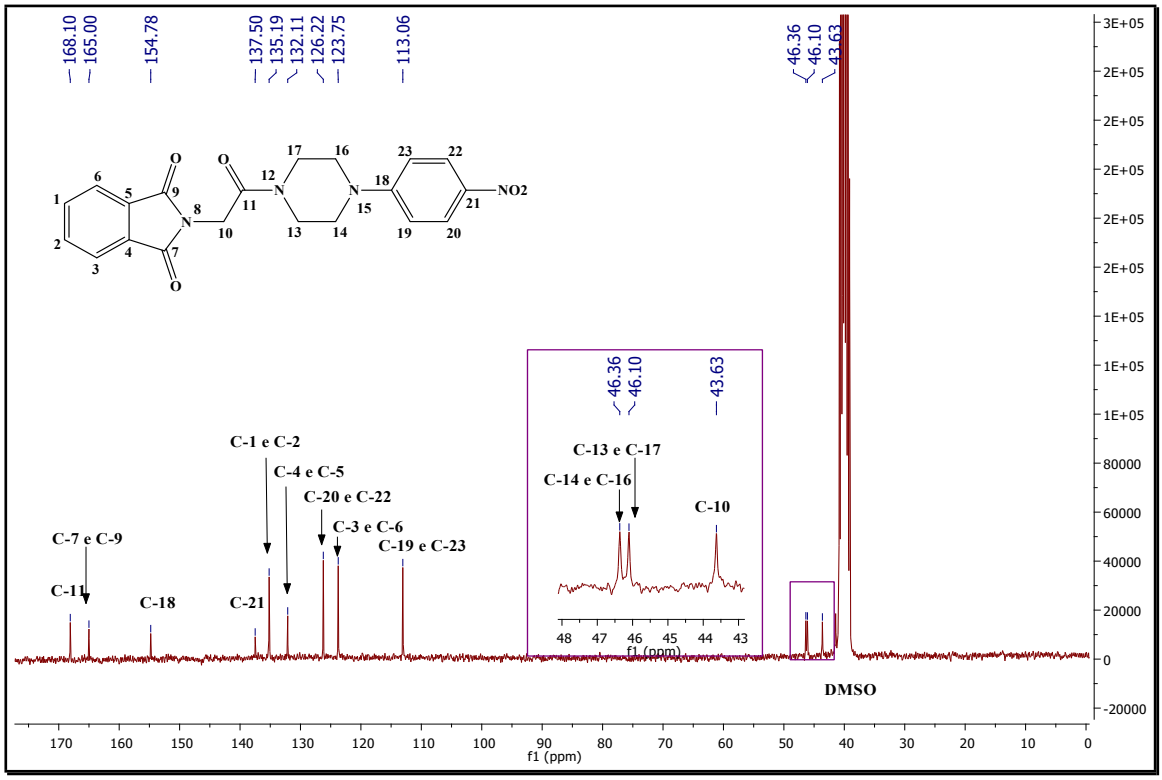

Figure 31. ^{13}C NMR spectra of *2-(2-(4-(4-nitrophenyl)piperazin-1-yl)-2-oxoethyl)isoindoline-1,3-dione* **(3h)** (75 MHz, DMSO).

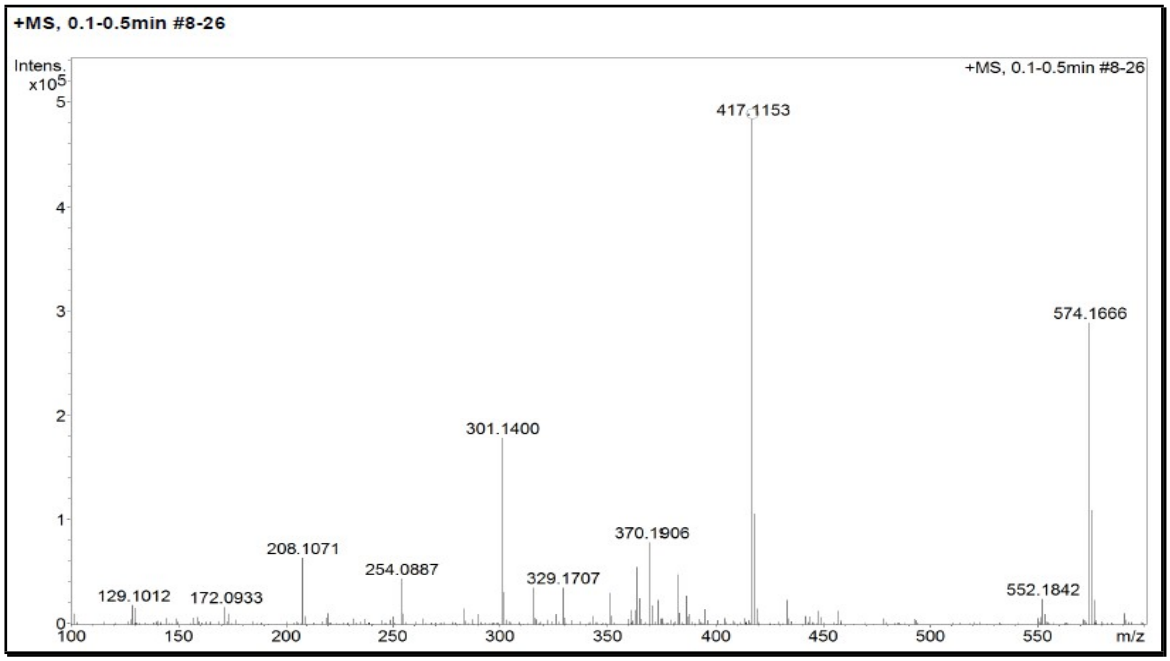

Figure 32. HR-MS spectra of *2-(2-(4-(4-nitrophenyl)piperazin-1-yl)-2-oxoethyl)isoindoline-1,3-dione* **(3h)** (ESI-MS).

HPLC Chromatograms of compounds 3a-h

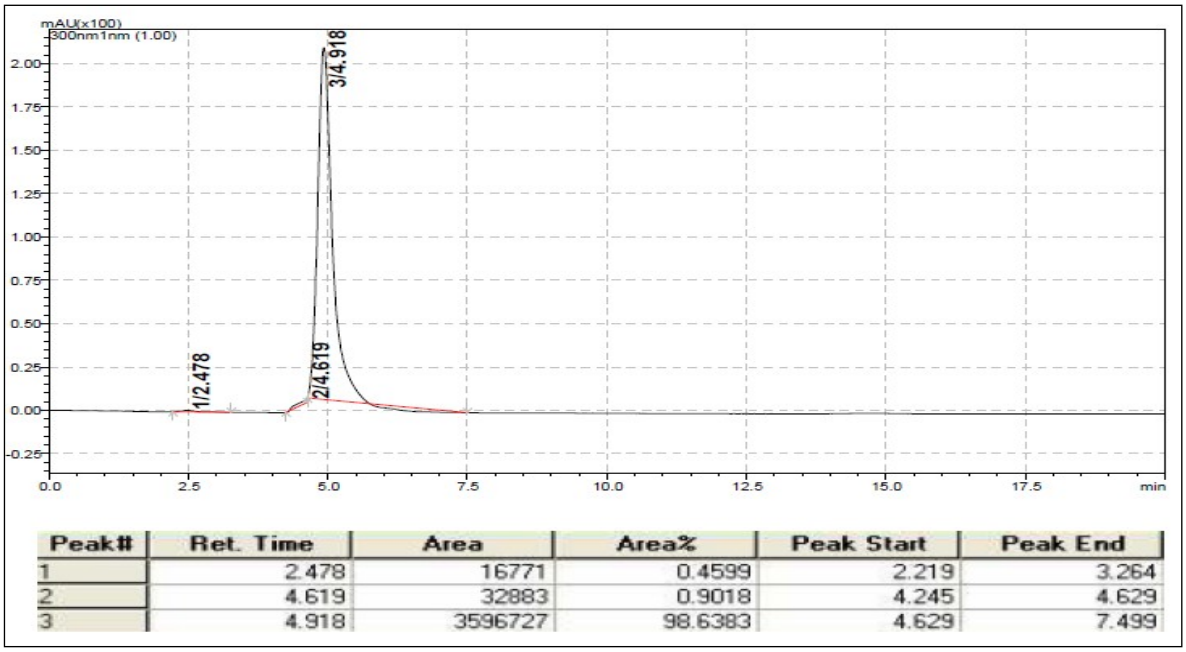

Peak#	Ret. Time	Area	Area%	Peak Start	Peak End
1	2.478	16771	0.4599	2.219	3.264
2	4.619	32883	0.9018	4.245	4.629
3	4.918	3596727	98.6383	4.629	7.499

Figure 33. HPLC chromatogram of compound *2-(2-(4-(4-bromobenzyl)piperazin-1-yl)-2-oxoethyl)isoindoline-1,3-dione* **(3a).**

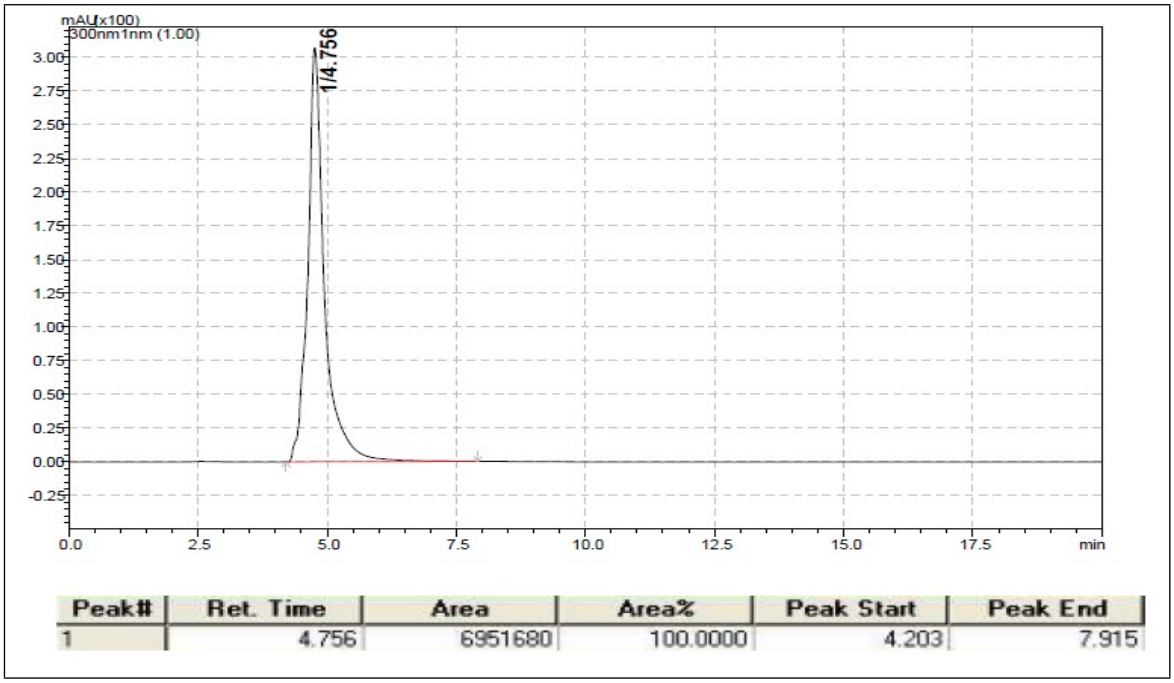

Peak#	Ret. Time	Area	Area%	Peak Start	Peak End
1	4.756	6951680	100.0000	4.203	7.915

Figure 34. HPLC chromatogram of compound *2-(2-oxo-2-(4-(p-tolyl)piperazin-1-yl)ethyl)isoindoline-1,3-dione* **(3b).**

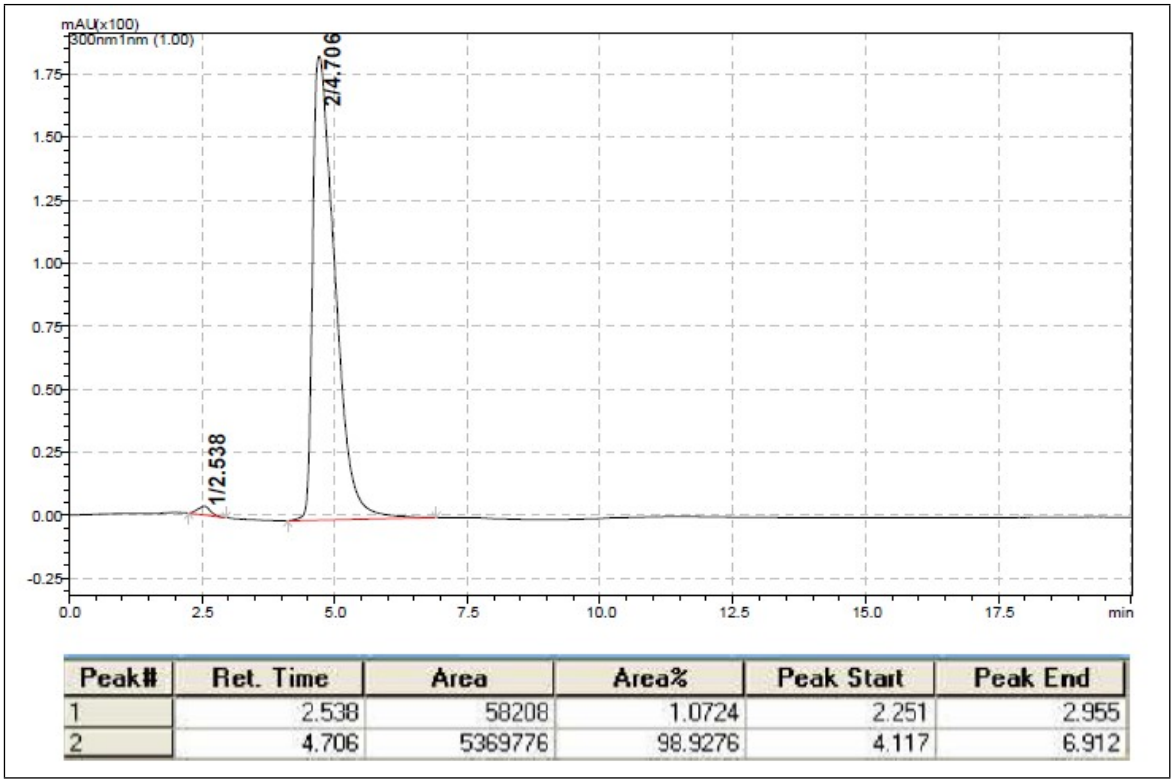

Peak#	Ret. Time	Area	Area%	Peak Start	Peak End
1	2.538	58208	1.0724	2.251	2.955
2	4.706	5369776	98.9276	4.117	6.912

Figure 35. HPLC chromatogram of compound *2-(2-oxo-2-(4-(pyrimidin-2-yl)piperazin-1-yl)ethyl)isoindoline-1,3-dione* **(3c).**

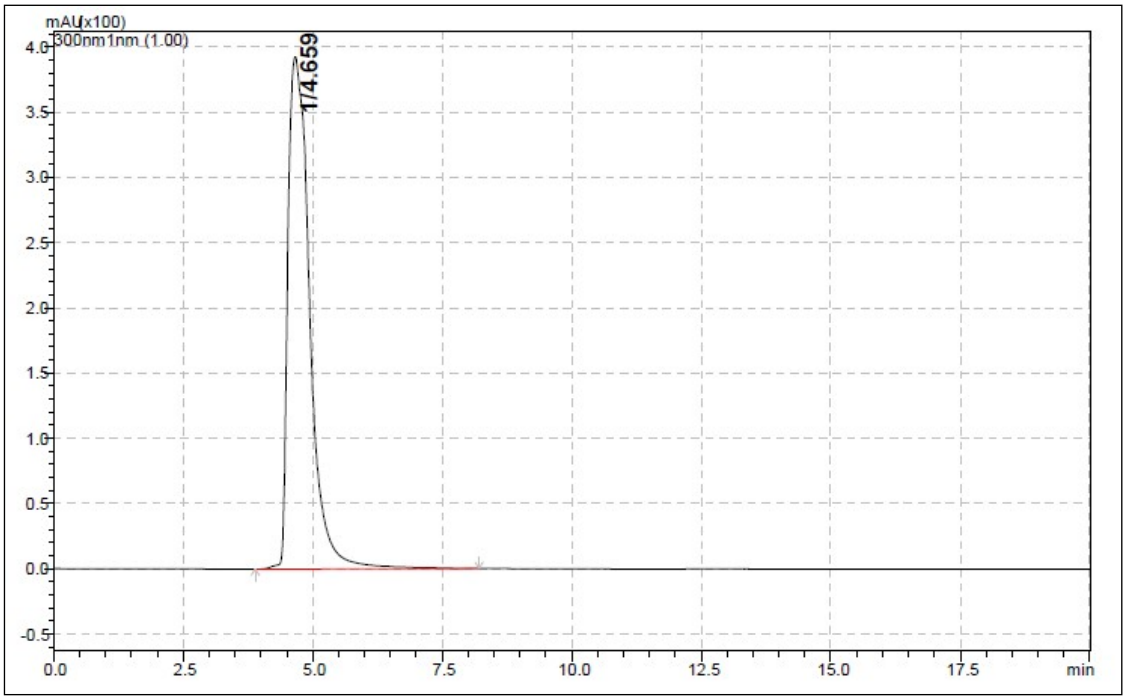

Figure 36. HPLC chromatogram of compound *2-(2-(4-(4-chlorophenyl)piperazin-1-yl)-2-oxoethyl)isoindoline-1,3-dione* **(3d).**

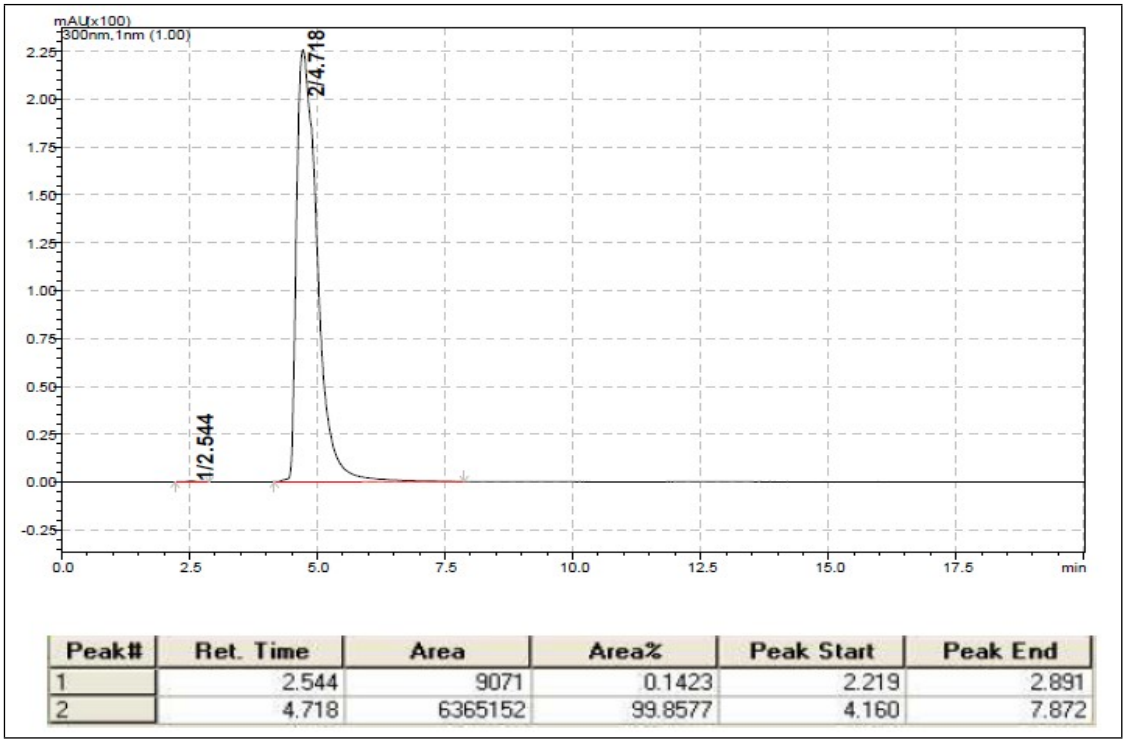

Peak#	Ret. Time	Area	Area%	Peak Start	Peak End
1	2.544	9071	0.1423	2.219	2.891
2	4.718	6365152	99.8577	4.160	7.872

Figure 37. HPLC chromatogram of compound *2-(2-(4-(4-methoxybenzyl)piperazin-1-yl)-2-oxoethyl)isoindoline-1,3-dione* **(3e).**

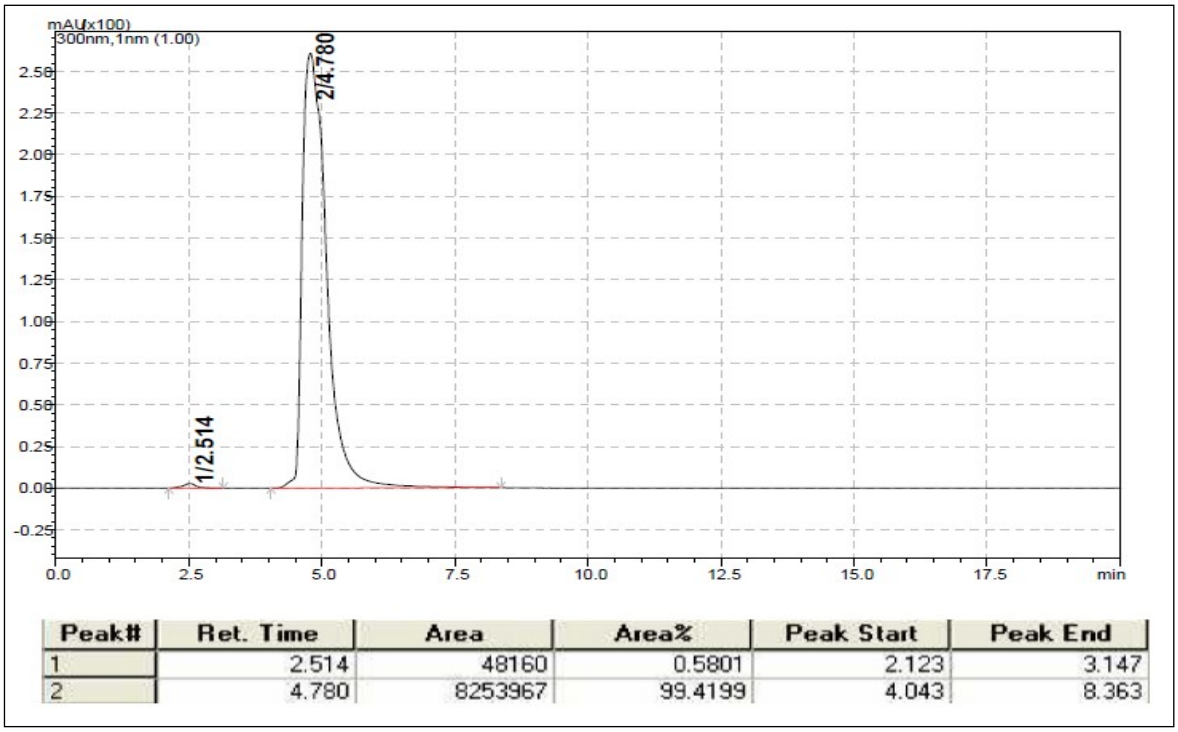

Peak#	Ret. Time	Area	Area%	Peak Start	Peak End
1	2.514	48160	0.5801	2.123	3.147
2	4.780	8253967	99.4199	4.043	8.363

Figure 38. HPLC chromatogram of compound *2-(2-(4-(4-chlorobenzyl)piperazin-1-yl)-2-oxoethyl)isoindoline-1,3-dione* **(3f).**

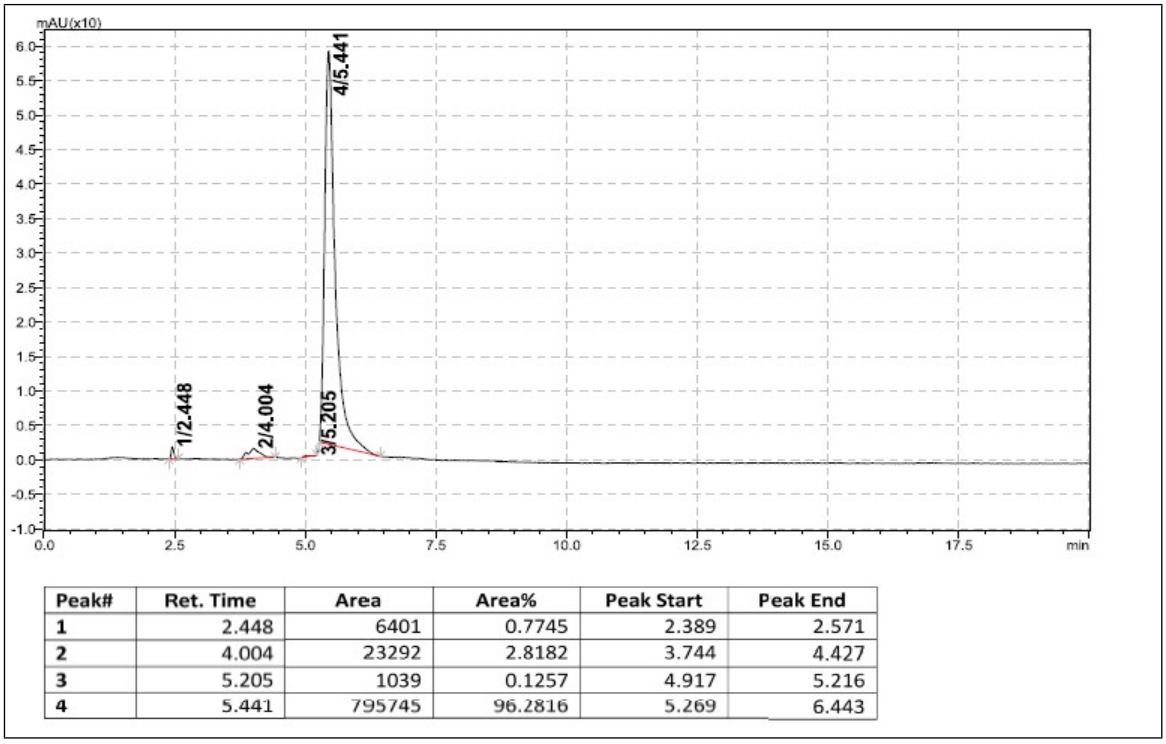

Peak#	Ret. Time	Area	Area%	Peak Start	Peak End
1	2.448	6401	0.7745	2.389	2.571
2	4.004	23292	2.8182	3.744	4.427
3	5.205	1039	0.1257	4.917	5.216
4	5.441	795745	96.2816	5.269	6.443

Figure 39. HPLC chromatogram of compound *2-(2-oxo-2-(4-(pyridin-4-yl)piperazin-1-yl)ethyl)isoindoline-1,3-dione* **(3g).**

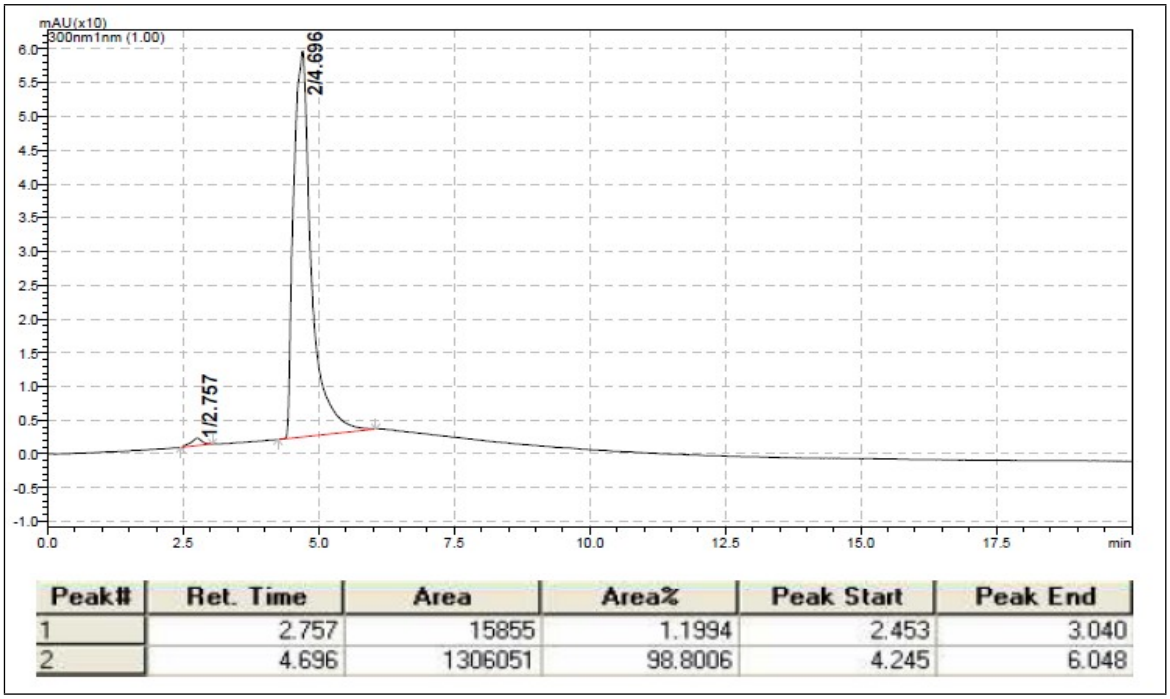

Peak#	Ret. Time	Area	Area%	Peak Start	Peak End
1	2.757	15855	1.1994	2.453	3.040
2	4.696	1306051	98.8006	4.245	6.048

Figure 40. HPLC chromatogram of compound *2-(2-(4-(4-nitrophenyl)piperazin-1-yl)-2-oxoethyl)isoindoline-1,3-dione* **(3h).**

. **In silico ADME data**

Table S1. *In silico* ADME data from QikProp v.3.5 software (Schrödinger) for the most active multitarget lead-compounds and donepezil

Compound	Molecular Volume[a]	QPlogPo/w[b]	QPlogS[c]	QPlogHERG[d]	QPlogBB[e]	QPlogKhsa[f]	QPPMDCK[g]	QPlogKp[h]	CNS[i]	% Absorção oral humano[j]	Human Oral Absorption[k]
PQM 183	1229,953	2,12	-2,935	-5,602	-0,31	-0,443	240,718	-4,257	1	77,158	3
PQM 184	1174,164	2,41	-4,341	-4,782	-0,847	-0,253	311,285	-2,566	-1	88,877	3
PQM 185	1098,222	1,099	-2,858	-4,726	-1,036	-0,874	186,166	-2,893	-2	77,51	3
PQM 186	1158,1	2,588	-4,498	-4,783	-0,663	-0,299	767,407	-2,535	0	89,921	3
PQM 187	1253,102	1,603	-2,212	-5,572	-0,561	-0,619	90,962	-4,185	1	74,139	3
PQM 188	1220,948	2,04	-2,814	-5,573	-0,318	-0,469	223,94	-4,254	1	76,695	3
PQM 189	1101,684	1,077	-2,822	-4,66	-1,084	-0,864	160,269	-3,009	-2	76,299	3
PQM 190	1189,395	1,345	-3,818	-4,831	-1,937	-0,518	30,981	-4,275	-2	66,051	3
Donepezil	1266.695	4,368	-4,477	-6,608	0,189	0,569	485,175	-2,921		100	3
Values of reference*	500.0 – 2000.0	-2 - 6.5	-6.5 - 0.5	< -5 (not good)	-3 - 1.2	-1.5 - 1.5	<25 poor, > 500 great	–8.0 – – 1.0	–2 - +2	<25% is Low	–1.5 – 1.5

*VR = gap or recommended value for 95% of known drugs (source: QikProp 3.2 Manual User – Schrödinger Software)

a: Total solvent-accessible volume in cubic angstroms using a probe with a 1.4 Å radius
b: Predicted octanol/water partition coefficient.
c: Predicted aqueous solubility, log S. S in mol dm^{-3} is the concentration of the solute in a saturated solution that is in equilibrium with the crystalline solid.
d: Predicted IC_{50} value for blockage of HERG K+ channels.
e: Predicted brain/blood partition coefficient. Note: QikProp predictions are for orally delivered drugs so, for example, dopamine and serotonin are CNS negative because they are too polar to cross the blood-brain barrier
f: Prediction of binding to human serum albumin.
g: Predicted apparent MDCK cell permeability in nm/sec. MDCK cells are considered to be a good mimic for the blood-brain barrier. QikProp predictions are for non-active transport
h: Predicted skin permeability, log *K*p.
i: Predicted central nervous system activity on a –2 (inactive) to +2 (active) scale.
j: Predicted human oral absorption on 0 to 100% scale.
k: Predicted qualitative human oral absorption: 1, 2, or 3 for low, medium, or high.

PAMPA BBB assay

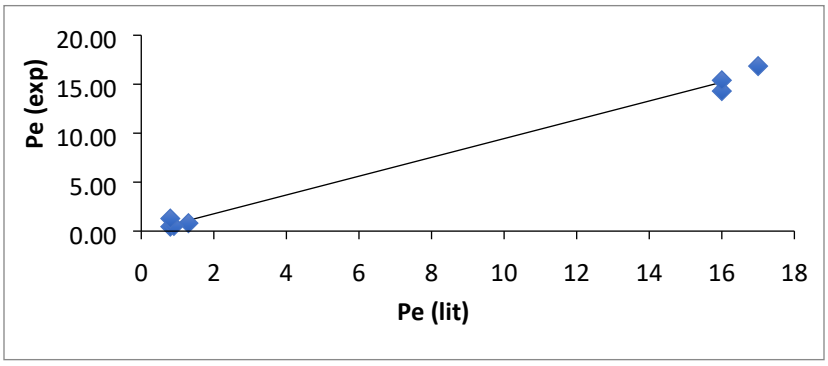

Figure 41. Linear correlation between experimental and literature permeability (Pe) values. Data represent the mean of triplicates in two different analyzes (n=2).

Table S2. Permeability coefficient of standard drugs used as control and target compound by the PAMPA-BBB technique. Values of cLog BB and cLog P calculated in silico by the ACD/Percepta Program.

Compound	*Pe* literature (10^{-6} cm s^{-1})	*Pe* experimental (10^{-6} cm s^{-1})	Classification	cLog BB	cLog P	PSA
Atenolol	0,8	0,46	CNS -	-	-	-
Caffeine	1,3	0,81	CNS -	-	-	-
Diazepam	16	14,30	CNS +	-	-	-
Enoxacine	0,9	0,53	CNS -	-	-	-
Ofloxacin	0,8	1,29	CNS -	-	-	-
Testosterone	17	16,85	CNS +	-	-	-
Verapamil	16	15,40	CNS +	-	-	-
PQM-189	-	13,89	CNS +	-0,77	2,40	60,93

PAMPA BBB assay

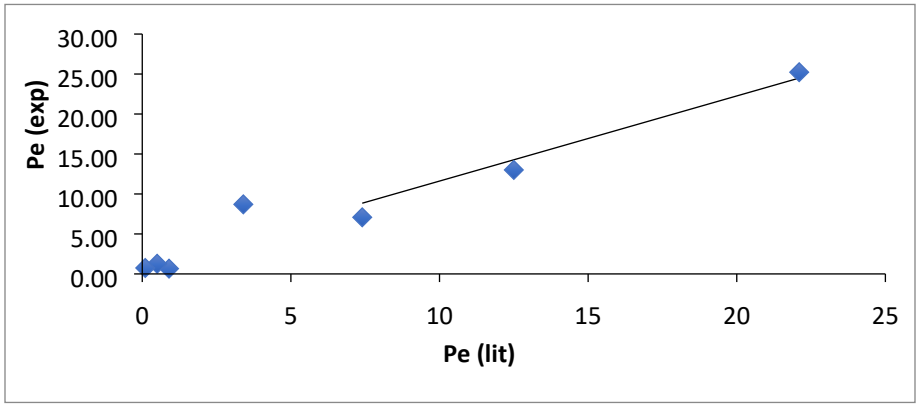

Figure 42. Linear correlation between experimental and literature permeability (Pe) values. Data represent the mean of triplicates in two different analyzes (n=2).

Table S3. Permeability coefficient of standard drugs, used as control, and target compound by the PAMPA-TGI technique. cLog P values calculated in silico by the ACD/Percepta Program.

Compound	Pe literature (10^{-6} cm s^{-1})	Pe experimental (10^{-6} cm s^{-1})	Fa (%)	Classification	cLog P	PSA
Acyclovir	**0**	0,05	1,70	low	-1,75	56,16
Atenolol	**0**	0,06	2,26	low	-1,15	75,16
Ceftriaxone	**0**	0,01	0,37	low	-1,41	159,08
Coumarin	**22,1**	25,23	99,99	low	0,51	21,63
Diclofenac	**12,5**	13,01	99,28	High	-0,25	39,83
Hydrocortisone	**3,4**	8,70	96,34	high	1,99	73,98
Norfloxacin	**0,9**	0,66	22,19	low	-1,59	61,13
Ranitidine	**0,5**	1,27	38,29	medium	-1,93	58,34
Sulfasalazine	**0,1**	0,75	24,66	low	-0,86	117,78
Verapamil	**7,4**	7,08	93,22	high	0,69	38,18
PQM-189	-	3,15	69,80	medium	2,40	60,93